Early View

Original research article

Urinary metabotype of severe asthma evidences decreased carnitine metabolism independent of oral corticosteroid treatment in the U-BIOPRED study

Stacey N. Reinke, Shama Naz, Romanas Chaleckis, Hector Gallart-Ayala, Johan Kolmert, Nazanin Z. Kermani, Angelica Tiotiu, David I. Broadhurst, Anders Lundqvist, Henric Olsson, Marika Ström, Åsa M. Wheelock, Cristina Gómez, Magnus Ericsson, Ana R. Sousa, John H. Riley, Stewart Bates, James Scholfield, Matthew Loza, Frédéric Baribaud, Per S. Bakke, Massimo Caruso, Pascal Chanez, Stephen J. Fowler, Thomas Geiser, Peter Howarth, Ildikó Horváth, Norbert Krug, Paolo Montuschi, Annelie Behndig, Florian Singer, Jacek Musial, Dominick E. Shaw, Barbro Dahlén, Sile Hu, Jessica Lasky-Su, Peter J. Sterk, Kian Fan Chung, Ratko Djukanovic, Sven-Erik Dahlén, Ian M. Adcock, Craig E. Wheelock

Urinary metabotype of severe asthma evidences decreased carnitine metabolism independent of oral corticosteroid treatment in the U-BIOPRED Study

Stacey N. Reinke[1,2,†], Shama Naz[1,†], Romanas Chaleckis[1,3], Hector Gallart-Ayala[1], Johan Kolmert[1,4], Nazanin Z. Kermani[5], Angelica Tiotiu[5,6], David I. Broadhurst[2], Anders Lundqvist[7], Henric Olsson[8] Marika Ström[9,10], Åsa M. Wheelock[9,10], Cristina Gómez[1,4], Magnus Ericsson[11], Ana R. Sousa[12], John H. Riley[12], Stewart Bates[12], James Scholfield[13], Matthew Loza[14], Frédéric Baribaud[14], Per S. Bakke[15], Massimo Caruso[16], Pascal Chanez[17], Stephen J. Fowler[18], Thomas Geiser[19], Peter Howarth[13], Ildikó Horváth[20], Norbert Krug[21], Paolo Montuschi[22], Annelie Behndig[23], Florian Singer[24], Jacek Musial[25], Dominick E. Shaw[26], Barbro Dahlén[10], Sile Hu[27], Jessica Lasky-Su[28], Peter J. Sterk[29], Kian Fan Chung[5], Ratko Djukanovic[13], Sven-Erik Dahlén[4,10], Ian M. Adcock[5], *Craig E. Wheelock[1,3,10], on behalf of the U-BIOPRED Study Group#

Affiliations:
1) Division of Physiological Chemistry 2, Department of Medical Biochemistry and Biophysics, Karolinska Institute, Stockholm, Sweden.
2) Centre for Integrative Metabolomics & Computational Biology, School of Science, Edith Cowan University, Perth, Australia
3) Gunma Initiative for Advanced Research (GIAR), Gunma University, Maebashi, Japan
4) The Institute of Environmental Medicine, Karolinska Institutet, Stockholm, Sweden
5) National Heart and Lung Institute, Imperial College, London, U.K.
6) Department of Pulmonology, University Hospital of Nancy, Nancy, France
7) DMPK, Research and Early Development, Respiratory & Immunology, BioPharmaceuticals R&D, AstraZeneca, Gothenburg, Sweden
8) Translational Science and Experimental Medicine, Research and Early Development, Respiratory & Immunology, BioPharmaceuticals R&D, AstraZeneca, Gothenburg, Sweden
9) Respiratory Medicine Unit, K2 Department of Medicine Solna and Center for Molecular Medicine, Karolinska Institutet, Stockholm, Sweden
10) Department of Respiratory Medicine and Allergy, Karolinska University Hospital, Stockholm, Sweden
11) Department of Clinical Pharmacology, Huddinge Campus, Karolinska Institutet and Karolinska University Hospital, Stockholm, Sweden
12) Glaxo Smith Kline, London, U.K.
13) Faculty of Medicine, Southampton University and NIHR Southampton Respiratory Biomedical Research Center, University Hospital Southampton, Southampton, U.K.
14) Janssen Research and Development, High Wycombe, U.K.
15) Institute of Medicine, University of Bergen, Bergen, Norway
16) Department of Biomedical and Biotechnological Sciences and Department of Clinical and Experimental Medicine, University of Catania, Catania, Italy
17) Assistance Publique des Hôpitaux de Marseille, Clinique des Bronches, Allergies et Sommeil, Aix Marseille Université, Marseille, France

18) Division of Infection, Immunity and Respiratory Medicine, School of Biological Sciences, Faculty of Biology, Medicine and Health, University of Manchester, and Manchester Academic Health Science Centre and NIHR Biomedical Research Centre, Manchester University Hospitals NHS Foundation Trust, Manchester, U.K.
19) Department of Pulmonary Medicine, University Hospital, University of Bern, Switzerland
20) Department of Pulmonology, Semmelweis University, Budapest, Hungary
21) Fraunhofer Institute for Toxicology and Experimental Medicine, Hannover, Germany
22) Pharmacology, Catholic University of the Sacred Heart, Rome, Italy
23) Department of Public Health and Clinical Medicine, Section of Medicine, Umeå University, Umeå, Sweden
24) Division of Paediatric Respiratory Medicine and Allergology, Department of Paediatrics, Inselspital, Bern University Hospital, University of Bern, Switzerland
25) Dept of Medicine, Jagiellonian University Medical College, Krakow, Poland
26) Nottingham NIHR Biomedical Research Centre, University of Nottingham, U.K.
27) Data Science Institute, Imperial College, London, U.K.
28) Channing Division of Network Medicine, Brigham and Women's Hospital and Harvard Medical School, Boston, MA, USA
29) Department of Respiratory Medicine, Amsterdam UMC, University of Amsterdam, Amsterdam, The Netherlands

†equal contribution

*corresponding author
Craig E Wheelock
Division of Physiological Chemistry 2
Department of Medical Biochemistry and Biophysics
Karolinska Institutet
Solnavägen 9, Biomedicum Quartier 9A
171 77 Stockholm, Sweden
Telephone: +46-852487630
Email: craig.wheelock@ki.se

Funding

Abstract

Introduction

Asthma is a heterogeneous disease with poorly defined phenotypes. Severe asthmatics often receive multiple treatments including oral corticosteroids (OCS). Treatment may modify the observed metabotype, rendering it challenging to investigate underlying disease mechanisms. Here, we aimed to identify dysregulated metabolic processes in relation to asthma severity and medication.

Methods

Baseline urine was collected prospectively from healthy participants (n=100), mild-to-moderate asthmatics (n=87) and severe asthmatics (n=418) in the cross-sectional U-BIOPRED cohort; 12-18-month longitudinal samples were collected from severe asthmatics (n=305). Metabolomics data were acquired using high-resolution mass spectrometry and analysed using univariate and multivariate methods.

Results

Ninety metabolites were identified, with 40 significantly altered ($p<0.05$, FDR<0.05) in severe asthma and 23 by OCS use. Multivariate modelling showed that observed metabotypes in healthy participants and mild-to-moderate asthmatics differed significantly from severe asthmatics ($p=2.6\times10^{-20}$), OCS-treated asthmatics differed significantly from non-treated ($p=9.5\times10^{-4}$), and longitudinal metabotypes demonstrated temporal stability. Carnitine levels evidenced the strongest OCS-independent decrease in severe asthma. Reduced carnitine levels were associated with mitochondrial dysfunction via decreases in pathway enrichment scores of fatty acid metabolism and reduced expression of the carnitine transporter SLC22A5 in sputum and bronchial brushings.

Conclusions

This is the first large-scale study to delineate disease- and OCS-associated metabolic differences in asthma. The widespread associations with different therapies upon the observed metabotypes demonstrate the necessity to evaluate potential modulating effects on a treatment- and metabolite-specific basis. Altered carnitine metabolism is a potentially actionable therapeutic target that is independent of OCS treatment, highlighting the role of mitochondrial dysfunction in severe asthma.

Take Home Message

The severe asthma urinary metabotype is distinct from healthy individuals and mild-to-moderate asthmatics. Observed metabotypes are modified in oral corticosteroid (OCS)-treated individuals; however, carnitine metabolism is downregulated in severe asthmatics independent of OCS. Findings suggest that carnitine metabolism is a potential therapeutic target in asthma management.

Tweet

Metabolomics identified a urinary metabotype of asthma driven by lower carnitine levels in an oral corticosteroid-independent manner. The carnitine transporter SLC22A5 was also decreased, suggesting carnitine metabolism as a potential therapeutic target.

Key words

asthma; metabolomics; metabolism; carnitine; mitochondria; corticosteroids

Introduction

Asthma is a heterogeneous inflammatory disease consisting of multiple phenotypes [1, 2]. Research has focused on identifying molecular descriptors of sub-groups in relation to clinical outcomes towards the aim of stratifying individuals for appropriate treatment strategies [3]. While it is ideal to interrogate the disease in the organ of manifestation, it is not feasible to perform routine sampling in the lung, especially in individuals with severe disease or at the population level. Accordingly, there is a need to identify molecular signatures in accessible biofluids (*e.g.,* blood, urine, exhaled breath condensate) that indicate pathophysiologically-driven biochemical perturbations. Urine has been successfully used to investigate local physiology in the lung [4] and is well-suited to clinical applications due to accessibility and ease of collection.

Mass spectrometry-based metabolomics in blood and urine has identified molecular signatures associated with both adult [5] and paediatric [6] asthma. In particular, metabolomics has detected metabolic signatures associated with aspirin-exacerbated respiratory disease [7], disease severity [8-10], bronchodilator response [11], pulmonary function [12], exacerbation [13], and corticosteroid resistance [14]. While these investigations have provided insight into metabolic dysregulation in association with disease, they have generally focused on smaller cohorts with little information on the longitudinal stability of the observed metabotypes [5, 14]. Furthermore, the potential modulating effects of asthma treatment on the observed metabotypes have not been evaluated. Oral corticosteroid (OCS) treatment is of particular interest as long-term OCS use is associated with multiple side effects including osteoporosis, adrenal suppression, metabolic disorders, psychiatric disorders, and infection [15].

We hypothesise that systemic therapies such as oral corticosteroids (OCS) as well as disease severity are reflected in the urinary metabolome. Using the U-BIOPRED (Unbiased Biomarkers for the Prediction of Respiratory Disease outcomes) study [16], we demonstrate that urinary metabotypes of severe asthma are dysregulated relative to healthy individuals, stable for 12-18 months, and susceptible to associations with asthma medication on a metabolite-specific basis.

Methods

Study subjects and design

Urine samples were prospectively collected for the cross-sectional U-BIOPRED study [16]; all available samples were included in the present study (**Table 1**). Participants were classified according to international guidelines into the following groups: healthy participants (n=100), mild-to-moderate asthmatics (n=87), non-smoking severe asthmatics (n=310), and smoking/ex-smoking severe asthmatics (n=108) [16]. Non-smokers were defined as participants being never smokers or non-smokers for at least 12 months prior to recruitment with a smoking history of less than 5 pack-years. Participants provided a urine sample within 28 days of initial screening (baseline visit); an additional urine sample was provided by 305 participants with severe asthma at a 12-18-month longitudinal visit. An overview of participant characteristics is shown in **Table 1**, with a detailed description provided elsewhere [16]. Ethics approval was obtained from each clinical institution and all participants provided written informed consent (ClinicalTrials.gov identifier: NCT01976767).

Treatment use and stratification

Treatment use and stratification protocols are presented in detail in the online supplement and have been reported previously [4]. Briefly, all mild-to-moderate asthmatics were on ≤500 μg inhaled fluticasone equivalents/day (ICS), while severe asthmatics received ≥1000 μg fluticasone equivalents/day [16]. Reliever medication, such as short/long acting β_2 agonists (SABA/LABA) or combination therapy, was used by all asthmatic subjects. Severe asthma non-smokers were stratified based upon treatment where use could be confirmed (OCS, omalizumab), and/or existing literature provides evidence for a confounding effect on the metabolome (OCS, theophylline) [8, 9, 17-19], and/or a sufficient proportion of the individuals received treatment in order to render stratification meaningful (anticholinergics, leukotriene modifiers).

Mass spectrometry analysis

Metabolomics data were acquired by liquid chromatography–high resolution mass spectrometry (LC-HRMS) using previously published methods [20] that enabled detection of hydrophilic metabolites. Urine dilution was normalised to specific gravity prior to data acquisition [21]. Detailed methods are provided in the supplementary material. Tryptophan and 6 of its metabolites were quantified by reversed-phase liquid chromatography coupled to tandem mass spectrometry (LC-MS/MS) as described in the supplementary material.

Transcriptomics and Genotyping

Bronchial brushings [22], sputum [23], and peripheral blood mononuclear cells (PBMCs) [24] were collected and transcriptomics analyses performed as previously

described. Bronchial bushings and sputum samples were genotyped on the Affymetrix Axiom® UK Biobank array [25].

Statistical analysis

Metabolomics data were not normally distributed (Lilliefors test); non-parametric univariate statistical tests were subsequently used. The Storey positive false discovery rate (FDR) [26] was calculated for all univariate analyses. Median fold-changes and confidence intervals were estimated using bootstrap resampling [8].

To identify similarities between metabolites, hierarchical cluster analysis (HCA) was performed. The mean of the log-transformed and z-scaled data of the resulting clusters were plotted against clinical groups to qualitatively visualise metabolite patterns across clinical groups. Multivariate Principal Components–Canonical Variate Analysis (PC-CVA) was performed [8], to assess the multifactorial and correlated discrimination between clinical groups. Kyoto Encyclopedia of Genes and Genomes (KEGG) pathway mapping was performed using gene set variation analysis (GSVA) enrichment score (ES) determination of the genes identified as being part of the fatty acid metabolism pathway. The Type-2 patient stratification was based on the ES of the IL-13-induced gene expression patterns in human bronchial epithelial cells using GSVA [23, 27], and transcriptome-associated cluster (TAC) membership was assigned based upon previous work [23]. Participant clinical and biochemical data were collected from the U-BIOPRED TranSMART platform (eTRIKS). All statistical analyses were performed using MATLAB (Mathworks, Natick, MA, USA).

Results

The identities of 90 urinary metabolites were confirmed against an in-house metabolite library. Using an FDR of 0.05, 40 metabolites were significantly ($p<0.05$) altered between the four study groups based on univariate analysis. Fold changes compared to healthy participants and all statistics (including *post hoc* pairwise group comparisons) are presented in **Table E1**.

Clustering of correlated metabolites

Hierarchical cluster analysis identified 7 metabolite clusters, revealing different metabolite abundance patterns across the four study groups (**Figure 1**). Cluster A was comprised of 20 metabolites, 6 of which were significant by univariate analysis (k=20; k=6, $p<0.05$). Both Clusters A and B (k=15; k=10, $p<0.05$) consisted primarily of amino acid metabolites and showed lower abundances in the severe asthmatics compared to the healthy participants and mild-to-moderate asthmatics. Cluster C (k=3, $p<0.05$) included carnitines, which decreased linearly with disease severity in the non-smoking groups. Severe asthma smokers showed elevated carnitine levels compared to non-smokers. Cluster D (k=20; k=9, $p<0.05$) included diverse metabolite classes: amino acid metabolites, organic acids, biogenic amines, and purine nucleosides that increased with disease severity and also with smoking status in severe asthma. Cluster E (k=6; k=2, $p<0.05$) consisted of purine metabolites, methylthioadenosine, and phosphoethanolamine; all groups exhibited similar abundances. In Clusters F (k=7; k=5, $p<0.05$) and G (k=19; k=5, $p<0.05$), healthy participants and mild-to-moderate asthmatics had similar levels, with severe asthmatics showing higher abundances. These clusters represented dietary and drug metabolites, with Cluster F

consisting of caffeine metabolites and Cluster G containing sugars, gut microbial metabolites, and other dietary products.

All clusters, except for E, qualitatively demonstrated temporal metabolic stability of non-smoking severe asthma, with metabolite levels at the 12-to-18-month longitudinal timepoint unchanged relative to the baseline values. Univariate analysis showed that 4 Cluster E metabolites (7-methylguanine, phosphoethanolamine, uric acid, xanthine) had a significantly different distribution (p<0.05) between baseline and longitudinal timepoints (**Table E2**).

Multivariate analysis

PC-CVA supported the hierarchical clustering and univariate findings (**Figure E1A**) and identified correlated metabolic drivers of severe asthma not revealed by these analyses. The first canonical variate (CV1) showed that the severe asthma groups were highly significantly different from the healthy participants and mild-to-moderate asthma groups ($p=2.6 \times 10^{-20}$). A total of 46 metabolites significantly ($p<0.05$) contributed to this mean group difference (**Figure E1C**), 27 of which were also univariately significant ($p<0.05$, **Table E1**). Metabolites that most strongly drove this separation included short-chain acylcarnitines, histidine, taurine, uracil, 2-deoxyinosine, and kynurenic acid (decreased in severe asthma), and sugars, proline, serotonin, N-methyl-D-aspartate (NMDA), glutamate, N-acetylputrescine, and 5-hydroxyindole acetic acid (increased in severe asthma) (**Figure E1C**). When projected through the model, the mean scores (with 95% confidence intervals) of the longitudinal groups overlapped with the respective baseline groups (**Figure E1B**), further demonstrating temporal metabolic stability at the 12-to-18-month longitudinal visit.

Treatment effects upon the urinary metabolome

To delineate between metabolic dysregulation associated with disease and treatment (OCS, theophylline and omalizumab), severe asthmatics non-smokers were stratified based upon treatment (**Table 1**). Of the 90 metabolites reported, 23 (25%; **Table 2, Table E3**) were significantly different (p<0.05, FDR<0.05) between OCS-treated and non-treated severe asthmatic non-smokers. Of the 27 metabolites dysregulated in association with severe asthma by both univariate and multivariate analysis, 9 were altered in OCS-treated individuals (33%). Metabolite abundances in Clusters A (k=3), B (k=3), D (k=6), E (k=2), and G (k=9) were different between OCS-treated and non-treated individuals, while metabolites in Clusters C and F were not significantly affected.

Multivariate analysis using PC-CVA (**Figure 2**) corroborated the univariate findings. CV1 described a significant mean difference between healthy and severe asthma participants (p=7.8×10^{-12}). CV2 described a significant mean difference between OCS-treated and OCS-not treated severe asthmatic non-smokers (p=9.5×10^{-4}). Metabolites from Clusters A, B, and C were less abundant in severe asthmatics (**Figures 2C, 3**). Four of the six Cluster A and B metabolites were further reduced in OCS users. The carnitines (Cluster C) had the largest effect on the PC-CVA model (**Figures 2C, 3**) and were not altered in the OCS-treated group. While metabolites in Cluster D were increased in severe asthmatics (**Figure 2C**), further inspection revealed that the increases for all metabolites except for glutamate were associated with OCS treatment, independent of asthma diagnosis (**Table 2**). Conversely, the Cluster D metabolite glutamate and all Cluster E metabolites were elevated in severe asthmatics

(**Figure 2C**) and decreased in the OCS-treated individuals (**Table 2**). The combined multivariate response showed that Cluster G metabolites were uniquely elevated in OCS-treated individuals (**Figure 2C**); univariate analysis showed varied associations with disease and OCS use (**Table 2**). Projection of longitudinal metabolite profiles into the multivariate model (**Figure 2B**) showed temporal stability for the OCS-treated group, but less stability for the non-treated group. Two Cluster E metabolites (phosphoethanolamine, $p=0.0043$; uric acid, $p=0.016$) were significantly different between the two time points.

The abundances of 4 metabolites were significantly different ($p<0.05$, FDR<0.05) between theophylline-treated and non-treated severe asthmatic non-smokers (**Table E4**); these included metabolites from Clusters A ($k=1$), B ($k=1$), and F ($k=2$). PC-CVA multivariate analysis showed that while there is a mean difference between theophylline-treated and non-treated individuals, it is less pronounced than OCS effects (**Figures E3, E4**). Omalizumab treatment was associated with few differences in urinary metabotypes, with only 2 metabolites (3-methylxanthine, ornithine) being significantly different ($p<0.05$, FDR<0.05) between omalizumab-treated and IgE-matched non-omalizumab treated severe asthmatic non-smokers (**Table E5**). Anticholinergics (**Table E6**) and leukotriene modifiers (**Table E7**) were not associated with any significant differences ($p<0.05$, FDR<0.05) between users and non-users. **Table E8** provides fold change analysis for all metabolites significantly affected by at least one treatment or smoking.

Carnitine metabolism

The strongest observed metabolic shift in association with asthma severity was in the carnitines (Cluster C). Given that this alteration was independent of OCS treatment, it was explored in more detail. While urinary carnitine levels were lower in females relative to males, this effect was independent of asthma diagnosis (**Figure E5**). Confounder correction, which included sex, age, and BMI as predictor variables (**Table E9**), showed that the significantly reduced carnitine abundances observed in the severe asthmatic non-smoking group were independent of these potential confounders. In addition, the carnitine species were also evaluated for recruitment site bias and found to be independent of collection centre ($p>0.8$, **Figure E6**). The 3 carnitine species were then z-scaled and concatenated (**Figure 4A**), which further demonstrated a strong decrease in association with asthma severity ($p=4.0\times10^{-9}$).

We then examined carnitine metabolism using KEGG pathway enrichment scores (ES) for fatty acid β-oxidation, which decreased with asthma severity in sputum ($p=8.02\times10^{-6}$, **Figure 4B**), but did not change in bronchial brushings ($p=0.82$, data not shown). The ES for fatty acid metabolism also decreased with asthma severity in sputum ($p=6.29\times10^{-6}$, **Figure 4C**) and bronchial brushings ($p=0.08$, data not shown). In addition, expression of the carnitine transporter SLC22A5 gene was evaluated due to its known association with genetic risk of asthma [25, 28]. SLC22A5 expression decreased with asthma severity in sputum ($p=5.96\times10^{-5}$, **Figure 4D**) and bronchial brushings ($p=0.058$, **Figure 4E**), and correlated with lung function ($FEV_1\%$ predicted $r=0.416$, $p=2.2\times10^{-5}$; **Figure 5**). SCL22A5 levels were lower in bronchial brushings of Type-2 high individuals ($p=9.7\times10^{-4}$; **Figure E7D**), as was fatty acid metabolism ES ($p=0.038$; **Figure E7B**). Similar findings were observed in sputum (**Figure E7C**).

Stratification based upon previously published sputum transcriptome-associated clusters (TACs [23]) found that fatty acid metabolism ES (p=2.1x10^{-14}) and SCL22A5 levels (p=1.2x10^{-10}) in sputum were higher in paucigranulocytic individuals with milder disease (TAC3) (**Figure E8**). One SLC22A5 eQTL (rs2522051, T/C) was found in sputum (effect allele C: beta=0.234, SD=0.148, p=0.119; **Figure 5C**) and bronchial brushings (effect allele C: beta=0.138, SD=0.057, p=0.028; **Figure 5D**). With respect to allele T, the direction of rs2522051 increases the risk of asthma while decreasing the expression of SLC22A5, indicating that activating SLC22A5 may reduce the risk of asthma. However, these data should be interpreted with caution due to the low sample number.

Discussion

We identified distinct urinary metabotypes of individuals with severe asthma that demonstrated temporal stability over at least 12-18 months; however, the metabotypes were sensitive to common treatment modalities. Cluster C, the carnitine species, displayed the largest alteration in association with severe asthma and was the only metabolite cluster unaffected by treatment. Findings in both sputum and bronchial brushings supported the observed systemic dysregulation in carnitine metabolism. Reduced fatty acid metabolism, β-oxidation (in sputum), and levels of the carnitine transporter SLC22A5 in severe asthmatics further implicate carnitine and central energy metabolism dysregulation in asthma. Single nucleotide polymorphisms (SNPs) in SLC22A5 have been previously reported to affect asthma risk [25, 28] and we identified rs2522051 to be an SLC22A5 eQTL that increases asthma risk while decreasing SLC22A5 expression, in agreement with earlier work [29]. While the limited power warrant caution in the conclusions drawn, these findings suggest that there is

a genetic component to the observed carnitine dysregulation in severe asthma and support a link between genetic determinants and systemic carnitine levels.

Carnitine is a small water-soluble molecule that possesses important physiological roles including transport of fatty acids into the mitochondrial matrix for β-oxidation, while short-chain acylcarnitines (primarily acetylcarnitine) transport organic acids out of the mitochondria and peroxisomes [30, 31]. Beyond its role in β-oxidation, carnitine also acts as a free radical scavenger [32] and can reduce oxidative stress-induced apoptosis [33]. Carnitine deficiency has been reported to cause pathological symptoms [30]. For example, reduced carnitine levels can result in a concomitant decline in mitochondrial free CoA and increased acyl-CoA, which has been linked with progressive emphysema [33, 34]. Studies have also shown systemic carnitine reduction during and after paediatric asthma exacerbation [35] and plasma levels were reported to be reduced in a guinea pig model of allergic asthma [36]. Sex-specific differences in circulating carnitine levels have been previously established, with lower constitutive levels in women [37]. While we also observed this pattern, the magnitude of the decrease associated with severe asthma was similar in both sexes (**Figure E5C**). Lower carnitine levels in women have been linked to sex hormones [38], with post-menopausal hormone replacement therapy use shown to further decrease circulating carnitine levels [39], suggesting that carnitine metabolism may play a role in the known link between female sex hormones and lung disease [40, 41].

These observations collectively suggest that carnitine metabolism may represent an actionable therapeutic target. For example, experimental allergic asthma models show mitochondrial functional changes that are reversed by an anti-IL-4 monoclonal

antibody [42]. Conversely, inhibiting carnitine palmitoyl transferase 1 (CPT1), the rate-limiting enzyme for β-oxidation in the mitochondria, with etomoxir reduced fatty acid metabolism and enhanced IL-4 expression in a mouse model of multiple sclerosis [43]. Carnitine supplementation has shown beneficial effects in several diseases [30], with decreased C-reactive protein (CRP), IL-6, and TNF-α, and increased superoxide dismutase (SOD) reported in randomised control trials [44]. Carnitine supplementation attenuated the development of porcine pancreatic elastase-induced emphysema [33]. This study highlights the importance of carnitine and central energy biochemistry in asthma, especially given that these processes are non-responsive to OCS treatment. Central energy metabolism is known to drive immune cell activation, with glycolysis and the pentose phosphate pathway promoting pro-inflammatory responses and β-oxidation, and oxidative phosphorylation promoting anti-inflammatory responses [45]. The deterministic cause of the shifted metabolic response remains unclear, particularly as to whether the observed altered mitochondrial function is a consequence of the chronic tissue hypoxia in asthma or dysfunction at the level of the mitochondria. Because there is no definitive mechanistic insight into the aetiological role that carnitine plays in asthma, future studies are warranted to elucidate this as well as the potential therapeutic benefit of carnitine supplementation in asthma.

Because OCS treatment may modulate observed metabolite concentrations, we stratified severe asthmatics by historical prescription of OCS and objective quantification of urinary prednisone (**Table 2, Figures 2-3**). Over 25% of the observed metabolites were significantly different in the OCS-treated group (**Table 2**, **Figure 2**), demonstrating that OCS treatment is a significant confounder in metabolomics-based investigations. We directly investigated the metabolic differences of OCS treatment

alone or in association with asthma (**Figure 6**) and identified metabolites that were dysregulated with asthma and appeared to respond to OCS treatment. Cluster E metabolites (purines including uric acid, methylthioadenosine, phosphoethanolamine), as well as the Cluster D metabolite glutamate, increased with asthma and decreased to levels of healthy participants in association with OCS treatment (**Figure 2**). Glutamate is a strong NMDA receptor agonist that can promote excitotoxicity, cough hypersensitivity [46], and pulmonary hypertension [47]. Polyamines promote cell differentiation and proliferation as well as airway smooth muscle contraction in asthma [48]. Methylthioadenosine is a biproduct of polyamine synthesis; we recently reported its increase in the serum of severe asthmatics [8]. Methylthioadenosine is subsequently catabolised via purine metabolism to uric acid (independent of OCS), which drives Type-2-mediated inflammation in asthma [49]. These shifts agree with *in vitro* research showing that dexamethasone treatment reduces both polyamine and purine synthesis [50] and may provide insights into OCS mechanisms of action in treating asthma. While it remains unclear whether these metabolites responded to OCS treatment, they should be evaluated as candidate treatment efficacy biomarkers in future steroid interventional trials.

Several metabolites showed OCS-associated metabolic differences independent of asthma diagnosis (**Table 2**, **Figure 2**). N-acetylputrescine, NMDA, S-adenosylhomocysteine (Cluster D), and allantoin (Cluster G) only increased ($p < 0.05$) in the OCS-treated group (**Figure 6**). Allantoin is a non-enzymatic oxidation product of the purine catabolic product uric acid and marker of oxidative stress [51], while N-acetylputrescine is an intermediary breakdown product of polyamines. S-adenosylhomocysteine is the product of methyltransferase reactions and metabolically

linked to the aminopropyl reactions required for polyamine synthesis (**Figure 6**). NMDA, which is another methyltransferase product, is an alternate agonist to glutamate for NMDA receptors. It has been shown to elicit contractile responses in human airway smooth muscle cells *in vitro* [52] and, surprisingly, bronchorelaxation responses in the murine house dust mite model of asthma [53]. While the consequences of these observed differences are unclear, they warrant further investigation to improve our understanding of the metabolic effects of OCS treatment, as well as provide insight into possible links to treatment side effects.

A number of recent asthma metabolomics studies have reported altered caffeine metabolism [9, 17-19]. As theophylline is a caffeine metabolite, the potential confounding effects of theophylline treatment in these interpretations remains unclear. Here we show that theophylline treatment is associated with differences in caffeine metabolism (Cluster F) as well as amino acid metabolism (Cluster A), dietary metabolites (Cluster G), and uracil (**Table E4**). While the global metabolic differences associated with theophylline treatment are less pronounced than OCS treatment (**Figure E3**), these findings suggest that metabolomics studies should be interpreted cautiously in the absence of theophylline treatment data. Conversely, the limited metabolic differences observed in association with omalizumab and no differences in association with anticholinergics or leukotriene modifier treatment demonstrate the need to evaluate potential metabolic confounders on a treatment-by-treatment basis.

There is significant interest in the potential role of tryptophan and its metabolites in multiple inflammatory diseases [54] including obstructive lung disease [55]. While the downstream metabolites of tryptophan were dysregulated with asthma severity, the

magnitude of the alterations was modest (**Figure E9, Table E10**). The strongest observed changes were in the indoleamine 2,3-dioxygenase (IDO) pathway, which has previously been reported to be associated with allergic airway inflammation [55]. Interestingly, IDO1 mRNA levels were increased in bronchial brushings, sputum, and PBMCs (**Table E11**), suggesting an upregulation of this pathway that was reflected in the urinary metabotype and was temporally stable (discussed in the supplemental information). Thus, significant tryptophan dysregulation occurs in asthma, but its impact is minor.

The current study is unique and represents the only large-scale mass spectrometry-based investigation of the urinary metabolome in adult asthmatics performed to date. However, there are limitations to this study that should be considered. While the mass spectrometry method was untargeted, reported metabolites were limited to those with identifications confirmed by chemical standards. Accordingly, the availability of additional analytical standards could increase the number of identified metabolites. Although the observed metabotypes provided insight into disease mechanisms and treatment stratification, they did not possess sufficient molecular resolution to identify unbiased endotypes of severe asthma. While a particular strength is that we confirmed adherence to OCS medication, the observed association between OCS and metabolite levels raises the question of whether ICS and reliever medication (SABA/LABA) evidence similar effects. Because current use of ICS and SABA/LABA were inclusion criteria for all U-BIOPRED subjects, it was not possible to stratify asthmatics for these treatments. Future studies could investigate this question using a dose-dependent interventional design. Performing similar stratifications in other disease contexts (*e.g.,* inflammatory bowel disease, rheumatoid arthritis) could help

establish the effects of corticosteroid use on observed metabolism. However, it would be necessary to perform an intervention study to definitively describe the temporal and dose-response relationship between OCS treatment and observed metabotypes, and to identify metabolic biomarkers of treatment efficacy. It is also challenging to separate the effect of omalizumab upon the urinary metabolome versus the effect of the qualifying (atopic) phenotype. Lastly, it is important to highlight that it remains for future studies to determine if the consistent metabolite profiles discerned in this study relate to the systemic inflammation in asthma or to more local tissue inflammation.

We demonstrate that severe asthmatics possess a dysregulated systemic metabotype relative to healthy individuals that it is temporally stable up to 12-18 months. The observed metabolic shifts are modulated by asthma-related therapeutics on a metabolite- and treatment-specific basis. In the current study, OCS treatment was associated with a difference in 25% of the observed metabolites, further highlighting the importance of evaluating this confounder in molecular studies. Short chain carnitines represented the strongest metabolic signature associated with asthma severity, decreased in an OCS-independent manner and were temporally stable, providing a metabolic link to the mitochondrial dysfunction associated with severe asthma and presenting a potential therapeutic target in asthma management.

References

1.   Tyler SR, Bunyavanich S. Leveraging -omics for asthma endotyping. *J Allergy Clin Immunol* 2019: 144(1): 13-23.
2.   Papi A, Brightling C, Pedersen SE, Reddel HK. Asthma. *Lancet* 2018: 391(10122): 783-800.
3.   Kaur R, Chupp G. Phenotypes and endotypes of adult asthma: Moving toward precision medicine. *J Allergy Clin Immunol* 2019: 144(1): 1-12.
4.   Kolmert J, Gomez C, Balgoma D, Sjodin M, Bood J, Konradsen JR, Ericsson M, Thorngren JO, James A, Mikus M, Sousa AR, Riley JH, Bates S, Bakke PS, Pandis I, Caruso M, Chanez P, Fowler SJ, Geiser T, Howarth P, Horvath I, Krug N, Montuschi P, Sanak M, Behndig A, Shaw DE, Knowles RG, Holweg CTJ, Wheelock AM, Dahlen B, Nordlund B, Alving K, Hedlin G, Chung KF, Adcock IM, Sterk PJ, Djukanovic R, Dahlen SE, Wheelock CE, U-BIOPRED Study Group. Urinary Leukotriene E4 and Prostaglandin D2 Metabolites Increase in Adult and Childhood Severe Asthma Characterized by Type 2 Inflammation. A Clinical Observational Study. *Am J Respir Crit Care Med* 2021: 203(1): 37-53.
5.   Kelly RS, Dahlin A, McGeachie MJ, Qiu W, Sordillo J, Wan ES, Wu AC, Lasky-Su J. Asthma Metabolomics and the Potential for Integrative Omics in Research and the Clinic. *Chest* 2017: 151(2): 262-277.
6.   Turi KN, Romick-Rosendale L, Ryckman KK, Hartert TV. A review of metabolomics approaches and their application in identifying causal pathways of childhood asthma. *J Allergy Clin Immunol* 2018: 141(4): 1191-1201.
7.   Ban GY, Cho K, Kim SH, Yoon MK, Kim JH, Lee HY, Shin YS, Ye YM, Cho JY, Park HS. Metabolomic analysis identifies potential diagnostic biomarkers for aspirin-exacerbated respiratory disease. *Clin Exp Allergy* 2017: 47(1): 37-47.
8.   Reinke SN, Gallart-Ayala H, Gomez C, Checa A, Fauland A, Naz S, Kamleh MA, Djukanovic R, Hinks TS, Wheelock CE. Metabolomics analysis identifies different metabotypes of asthma severity. *Eur Respir J* 2017: 49(3).
9.   Comhair SA, McDunn J, Bennett C, Fettig J, Erzurum SC, Kalhan SC. Metabolomic Endotype of Asthma. *J Immunol* 2015: 195(2): 643-650.
10.   Kelly RS, Virkud Y, Giorgio R, Celedon JC, Weiss ST, Lasky-Su J. Metabolomic profiling of lung function in Costa-Rican children with asthma. *Biochim Biophys Acta Mol Basis Dis* 2017: 1863(6): 1590-1595.
11.   Kelly RS, Sordillo JE, Lutz SM, Avila L, Soto-Quiros M, Celedon JC, McGeachie MJ, Dahlin A, Tantisira K, Huang M, Clish CB, Weiss ST, Lasky-Su J, Wu AC. Pharmacometabolomics of Bronchodilator Response in Asthma and the Role of Age-Metabolite Interactions. *Metabolites* 2019: 9(9).
12.   Yu B, Flexeder C, McGarrah RW, 3rd, Wyss A, Morrison AC, North KE, Boerwinkle E, Kastenmuller G, Gieger C, Suhre K, Karrasch S, Peters A, Wagner GR, Michelotti GA, Mohney RP, Schulz H, London SJ. Metabolomics Identifies Novel Blood Biomarkers of Pulmonary Function and COPD in the General Population. *Metabolites* 2019: 9(4).
13.   Loureiro CC, Duarte IF, Gomes J, Carrola J, Barros AS, Gil AM, Bousquet J, Bom AT, Rocha SM. Urinary metabolomic changes as a predictive biomarker of asthma exacerbation. *J Allergy Clin Immunol* 2014: 133(1): 261-263 e261-265.
14.   Park YH, Fitzpatrick AM, Medriano CA, Jones DP. High-resolution metabolomics to identify urine biomarkers in corticosteroid-resistant asthmatic children. *J Allergy Clin Immunol* 2017: 139(5): 1518-1524 e1514.

15. Price D, Castro M, Bourdin A, Fucile S, Altman P. Short-course systemic corticosteroids in asthma: striking the balance between efficacy and safety. *Eur Respir Rev* 2020: 29(155).

16. Shaw DE, Sousa AR, Fowler SJ, Fleming LJ, Roberts G, Corfield J, Pandis I, Bansal AT, Bel EH, Auffray C, Compton CH, Bisgaard H, Bucchioni E, Caruso M, Chanez P, Dahlen B, Dahlen SE, Dyson K, Frey U, Geiser T, Gerhardsson de Verdier M, Gibeon D, Guo YK, Hashimoto S, Hedlin G, Jeyasingham E, Hekking PP, Higenbottam T, Horvath I, Knox AJ, Krug N, Erpenbeck VJ, Larsson LX, Lazarinis N, Matthews JG, Middelveld R, Montuschi P, Musial J, Myles D, Pahus L, Sandstrom T, Seibold W, Singer F, Strandberg K, Vestbo J, Vissing N, von Garnier C, Adcock IM, Wagers S, Rowe A, Howarth P, Wagener AH, Djukanovic R, Sterk PJ, Chung KF, U-BIOPRED Study Group. Clinical and inflammatory characteristics of the European U-BIOPRED adult severe asthma cohort. *Eur Respir J* 2015: 46(5): 1308-1321.

17. McGeachie M, Kelly R, Litonjua A, Weiss S, Lasky-Su J. Network of Year-3 Metabolites Indicative of Early-Life Asthma. C26 PEDIATRIC ASTHMA: EPIDEMIOLOGY AND EPIGENETICS. American Thoracic Society, 2018; pp. A4606-A4606.

18. Kelly RS, Chawes BL, Blighe K, Virkud YV, Croteau-Chonka DC, McGeachie MJ, Clish CB, Bullock K, Celedon JC, Weiss ST, Lasky-Su JA. An Integrative Transcriptomic and Metabolomic Study of Lung Function in Children With Asthma. *Chest* 2018: 154(2): 335-348.

19. Liang Y, Gai XY, Chang C, Zhang X, Wang J, Li TT. Metabolomic Profiling Differences among Asthma, COPD, and Healthy Subjects: A LC-MS-based Metabolomic Analysis. *Biomed Environ Sci* 2019: 32(9): 659-672.

20. Naz S, Gallart-Ayala H, Reinke SN, Mathon C, Blankley R, Chaleckis R, Wheelock CE. Development of a Liquid Chromatography-High Resolution Mass Spectrometry Metabolomics Method with High Specificity for Metabolite Identification Using All Ion Fragmentation Acquisition. *Anal Chem* 2017: 89(15): 7933-7942.

21. Meister I, Zhang P, Sinha A, Skold CM, Wheelock AM, Izumi T, Chaleckis R, Wheelock CE. High-Precision Automated Workflow for Urinary Untargeted Metabolomic Epidemiology. *Anal Chem* 2021: 93(12): 5248-5258.

22. Kuo CS, Pavlidis S, Loza M, Baribaud F, Rowe A, Pandis I, Hoda U, Rossios C, Sousa A, Wilson SJ, Howarth P, Dahlen B, Dahlen SE, Chanez P, Shaw D, Krug N, Sandstrm T, De Meulder B, Lefaudeux D, Fowler S, Fleming L, Corfield J, Auffray C, Sterk PJ, Djukanovic R, Guo Y, Adcock IM, Chung KF, Team UBP. A Transcriptome-driven Analysis of Epithelial Brushings and Bronchial Biopsies to Define Asthma Phenotypes in U-BIOPRED. *Am J Respir Crit Care Med* 2017: 195(4): 443-455.

23. Kuo CS, Pavlidis S, Loza M, Baribaud F, Rowe A, Pandis I, Sousa A, Corfield J, Djukanovic R, Lutter R, Sterk PJ, Auffray C, Guo Y, Adcock IM, Chung KF, Group UBS. T-helper cell type 2 (Th2) and non-Th2 molecular phenotypes of asthma using sputum transcriptomics in U-BIOPRED. *Eur Respir J* 2017: 49(2).

24. Bigler J, Boedigheimer M, Schofield JPR, Skipp PJ, Corfield J, Rowe A, Sousa AR, Timour M, Twehues L, Hu X, Roberts G, Welcher AA, Yu W, Lefaudeux D, Meulder B, Auffray C, Chung KF, Adcock IM, Sterk PJ, Djukanovic R, Group UBS. A Severe Asthma Disease Signature from Gene Expression Profiling of Peripheral Blood from U-BIOPRED Cohorts. *Am J Respir Crit Care Med* 2017: 195(10): 1311-1320.

25. Shrine N, Portelli MA, John C, Soler Artigas M, Bennett N, Hall R, Lewis J, Henry AP, Billington CK, Ahmad A, Packer RJ, Shaw D, Pogson ZEK, Fogarty A, McKeever TM, Singapuri A, Heaney LG, Mansur AH, Chaudhuri R, Thomson NC,

Holloway JW, Lockett GA, Howarth PH, Djukanovic R, Hankinson J, Niven R, Simpson A, Chung KF, Sterk PJ, Blakey JD, Adcock IM, Hu S, Guo Y, Obeidat M, Sin DD, van den Berge M, Nickle DC, Bosse Y, Tobin MD, Hall IP, Brightling CE, Wain LV, Sayers I. Moderate-to-severe asthma in individuals of European ancestry: a genome-wide association study. *Lancet Respir Med* 2019: 7(1): 20-34.

26. Storey JD. A direct approach to false discovery rates. *Journal of the Royal Statistical Society: Series B (Statistical Methodology)* 2002: 64(3): 479-498.

27. Pavlidis S, Takahashi K, Ng Kee Kwong F, Xie J, Hoda U, Sun K, Elyasigomari V, Agapow P, Loza M, Baribaud F, Chanez P, Fowler SJ, Shaw DE, Fleming LJ, Howarth PH, Sousa AR, Corfield J, Auffray C, De Meulder B, Knowles R, Sterk PJ, Guo Y, Adcock IM, Djukanovic R, Fan Chung K, on behalf of the UBSG. "T2-high" in severe asthma related to blood eosinophil, exhaled nitric oxide and serum periostin. *Eur Respir J* 2019: 53(1).

28. Moffatt MF, Gut IG, Demenais F, Strachan DP, Bouzigon E, Heath S, von Mutius E, Farrall M, Lathrop M, Cookson W, Consortium G. A large-scale, consortium-based genomewide association study of asthma. *N Engl J Med* 2010: 363(13): 1211-1221.

29. Ferreira MAR, Mathur R, Vonk JM, Szwajda A, Brumpton B, Granell R, Brew BK, Ullemar V, Lu Y, Jiang Y, andMe Research T, e QC, Consortium B, Magnusson PKE, Karlsson R, Hinds DA, Paternoster L, Koppelman GH, Almqvist C. Genetic Architectures of Childhood- and Adult-Onset Asthma Are Partly Distinct. *Am J Hum Genet* 2019: 104(4): 665-684.

30. Flanagan JL, Simmons PA, Vehige J, Willcox MD, Garrett Q. Role of carnitine in disease. *Nutr Metab (Lond)* 2010: 7: 30.

31. Reuter SE, Evans AM. Carnitine and acylcarnitines: pharmacokinetic, pharmacological and clinical aspects. *Clin Pharmacokinet* 2012: 51(9): 553-572.

32. Selo MA, Sake JA, Ehrhardt C, Salomon JJ. Organic Cation Transporters in the Lung-Current and Emerging (Patho)Physiological and Pharmacological Concepts. *Int J Mol Sci* 2020: 21(23).

33. Conlon TM, Bartel J, Ballweg K, Gunter S, Prehn C, Krumsiek J, Meiners S, Theis FJ, Adamski J, Eickelberg O, Yildirim AO. Metabolomics screening identifies reduced L-carnitine to be associated with progressive emphysema. *Clin Sci (Lond)* 2016: 130(4): 273-287.

34. Halper-Stromberg E, Gillenwater L, Cruickshank-Quinn C, O'Neal WK, Reisdorph N, Petrache I, Zhuang Y, Labaki WW, Curtis JL, Wells J, Rennard S, Pratte KA, Woodruff P, Stringer KA, Kechris K, Bowler RP. Bronchoalveolar Lavage Fluid from COPD Patients Reveals More Compounds Associated with Disease than Matched Plasma. *Metabolites* 2019: 9(8).

35. Asilsoy S, Bekem O, Karaman O, Uzuner N, Kavukcu S. Serum total and free carnitine levels in children with asthma. *World J Pediatr* 2009: 5(1): 60-62.

36. Kertys M, Grendar M, Kosutova P, Mokra D, Mokry J. Plasma based targeted metabolomic analysis reveals alterations of phosphatidylcholines and oxidative stress markers in guinea pig model of allergic asthma. *Biochim Biophys Acta Mol Basis Dis* 2020: 1866(1): 165572.

37. Lambert ME, Shipley K, Holbrook I, Faragher EB, Irving MH. Serum carnitine levels in normal individuals. *JPEN J Parenter Enteral Nutr* 1988: 12(2): 143-146.

38. Ruoppolo M, Campesi I, Scolamiero E, Pecce R, Caterino M, Cherchi S, Mercuro G, Tonolo G, Franconi F. Serum metabolomic profiles suggest influence of sex and oral contraceptive use. *Am J Transl Res* 2014: 6(5): 614-624.

39.   Stevens VL, Wang Y, Carter BD, Gaudet MM, Gapstur SM. Serum metabolomic profiles associated with postmenopausal hormone use. *Metabolomics* 2018: 14(7): 97.

40.   Han MK, Arteaga-Solis E, Blenis J, Bourjeily G, Clegg DJ, DeMeo D, Duffy J, Gaston B, Heller NM, Hemnes A, Henske EP, Jain R, Lahm T, Lancaster LH, Lee J, Legato MJ, McKee S, Mehra R, Morris A, Prakash YS, Stampfli MR, Gopal-Srivastava R, Laposky AD, Punturieri A, Reineck L, Tigno X, Clayton J. Female Sex and Gender in Lung/Sleep Health and Disease. Increased Understanding of Basic Biological, Pathophysiological, and Behavioral Mechanisms Leading to Better Health for Female Patients with Lung Disease. *Am J Respir Crit Care Med* 2018: 198(7): 850-858.

41.   Tam A, Churg A, Wright JL, Zhou S, Kirby M, Coxson HO, Lam S, Man SF, Sin DD. Sex Differences in Airway Remodeling in a Mouse Model of Chronic Obstructive Pulmonary Disease. *Am J Respir Crit Care Med* 2016: 193(8): 825-834.

42.   Mabalirajan U, Dinda AK, Kumar S, Roshan R, Gupta P, Sharma SK, Ghosh B. Mitochondrial structural changes and dysfunction are associated with experimental allergic asthma. *J Immunol* 2008: 181(5): 3540-3548.

43.   Morkholt AS, Oklinski MK, Larsen A, Bockermann R, Issazadeh-Navikas S, Nieland JGK, Kwon TH, Corthals A, Nielsen S, Nieland JDV. Pharmacological inhibition of carnitine palmitoyl transferase 1 inhibits and reverses experimental autoimmune encephalitis in rodents. *PLoS One* 2020: 15(6): e0234493.

44.   Fathizadeh H, Milajerdi A, Reiner Ž, Amirani E, Asemi Z, Mansournia MA, Hallajzadeh J. The effects of L-carnitine supplementation on indicators of inflammation and oxidative stress: a systematic review and meta-analysis of randomized controlled trials. *J Diabetes Metab Disord* 2020: 1-16.

45.   Michaeloudes C, Bhavsar PK, Mumby S, Xu B, Hui CKM, Chung KF, Adcock IM. Role of Metabolic Reprogramming in Pulmonary Innate Immunity and Its Impact on Lung Diseases. *J Innate Immun* 2020: 12(1): 31-46.

46.   Chung KF. NMDA and GABA receptors as potential targets in cough hypersensitivity syndrome. *Curr Opin Pharmacol* 2015: 22: 29-36.

47.   Dumas SJ, Bru-Mercier G, Courboulin A, Quatredeniers M, Rucker-Martin C, Antigny F, Nakhleh MK, Ranchoux B, Gouadon E, Vinhas MC, Vocelle M, Raymond N, Dorfmuller P, Fadel E, Perros F, Humbert M, Cohen-Kaminsky S. NMDA-Type Glutamate Receptor Activation Promotes Vascular Remodeling and Pulmonary Arterial Hypertension. *Circulation* 2018: 137(22): 2371-2389.

48.   Jain V. Role of Polyamines in Asthma Pathophysiology. *Med Sci (Basel)* 2018: 6(1).

49.   Kool M, Willart MA, van Nimwegen M, Bergen I, Pouliot P, Virchow JC, Rogers N, Osorio F, Reis e Sousa C, Hammad H, Lambrecht BN. An unexpected role for uric acid as an inducer of T helper 2 cell immunity to inhaled antigens and inflammatory mediator of allergic asthma. *Immunity* 2011: 34(4): 527-540.

50.   Dyczynski M, Vesterlund M, Bjorklund AC, Zachariadis V, Janssen J, Gallart-Ayala H, Daskalaki E, Wheelock CE, Lehtio J, Grander D, Tamm KP, Nilsson R. Metabolic reprogramming of acute lymphoblastic leukemia cells in response to glucocorticoid treatment. *Cell Death Dis* 2018: 9(9): 846.

51.   Kaur H, Halliwell B. Action of biologically-relevant oxidizing species upon uric acid. Identification of uric acid oxidation products. *Chem Biol Interact* 1990: 73(2-3): 235-247.

52.   Anaparti V, Ilarraza R, Orihara K, Stelmack GL, Ojo OO, Mahood TH, Unruh H, Halayko AJ, Moqbel R. NMDA receptors mediate contractile responses in human airway smooth muscle cells. *Am J Physiol Lung Cell Mol Physiol* 2015: 308(12): L1253-1264.

53.   Anaparti V, Pascoe CD, Jha A, Mahood TH, Ilarraza R, Unruh H, Moqbel R, Halayko AJ. Tumor necrosis factor regulates NMDA receptor-mediated airway smooth muscle contractile function and airway responsiveness. *Am J Physiol Lung Cell Mol Physiol* 2016: 311(2): L467-480.

54.   Yeung AW, Terentis AC, King NJ, Thomas SR. Role of indoleamine 2,3-dioxygenase in health and disease. *Clin Sci (Lond)* 2015: 129(7): 601-672.

55.   Xu H, Oriss TB, Fei M, Henry AC, Melgert BN, Chen L, Mellor AL, Munn DH, Irvin CG, Ray P, Ray A. Indoleamine 2,3-dioxygenase in lung dendritic cells promotes Th2 responses and allergic inflammation. *Proc Natl Acad Sci U S A* 2008: 105(18): 6690-6695.

Table 1. Study characteristics of U-BIOPRED participants used for urinary metabolomics

	Baseline				Longitudinal	
	Healthy Controls	**Mild-to-Moderate Asthma**	**Severe Asthma non-smokers[1]**	**Severe Asthma ex/smokers**	**Severe Asthma non-smokers**	**Severe Asthma ex/smokers**
Subjects	100	87	310	108	225	80
Age years	35 (27-49)	43 (28-53)	53 (43-62)	55 (48-61)	55 (44-62)	55 (49-63)
Females	38 (38%)	43 (49%)	204 (68%)	56 (52%)	146 (65%)	37 (46%)
BMI kg/m^2	24.9 (22.8-27.5)	24.8 (23.0-28.8)	27.7 (24.6-33.6)	28.9 (25.1-32.6)	27.7 (24.5-33.3)	28.5(25.1-32.5)
FEV$_1$ % Pred (Pre-salbutamol)	101.8 (93.6-110.3)	91.6 (76.0-100.3)	67.4 (50.7-84.8)	66.2 (52.4-78.2)	67.85 (50.0-84.8)	60.4 (52.2-75.7)
FEV$_1$/FVC (Pre-salbutamol)	NA	72.7 (65.6-77.5)	63.4 (54.1-73.4)	60.1 (52.7-69.3)	62.2 (52.4-72.0)	60.8 (50.2-67.2)
FEV$_1$/FVC (Post-salbutamol)	NA	77.7 (72.0-83.1)	66.9 (56.9-77.4)	63.5 (54.8-72.6)	66.1 (54.4-76.0)	60.5 (53.8-68.9)
Exacerbations in previous year (n)	NA	0 (0-1)	2 (1-3)	2 (1-4)	2 (0-4)	1 (0-4)
Smoking history pack-years	0.9 (0.3-3.5)	4 (0.7-4.6)	2 (1-4)	17.1 (10-26)	NA	NA
Serum IgE IU·mL-1	23 (9-62)	89 (50-244)	117 (40-347)	122 (60-328)	NA	NA
Blood eosinophils x 10-3 ul-1	100 (90-200)	200 (100-300)	220 (110-405)	200 (100-405)	209 (100-401)	255 (148-450)
Sputum eosinophils %	0.4 (0.2-0.9)	1.3 (0.7-3.9)	4.5 (1.2-13.7)	4.1 (1.3-26.5)	1.8 (0.4-8.8)	3.2 (0.8-16.5)
FeNO ppb	19.5 (13.8-29)	25.5 (18-55)	22.5 (12-42)	26.5 (15.9-47.6)	24.0 (15.0-42.5)	20.8 (13.4-36.9)
Serum periostin ng·mL-1	49.7 (44.1-57.6)	48.3 (40.9-54.5)	43.8 (36.3-59.3)	49.7 (41.9-60.1)	51.7 (43.4-63.0)	48.8 (39.6-64.7)
hCRP mg·L-1	0.8 (0.4-1.6)	0.8 (0.4-2.1)	2.3 (1-4.8)	2.1 (0.9-4.8)	2 (0.8-4.9)	3.5 (1.4-6.0)
IL13 pg·mL-1	0.39 (0.28-0.62)	0.59 (0.4-0.86)	0.52 (0.3-1.11)	0.61 (0.31-1.14)	0.61 (0.31-1.23)	0.73 (0.36-1.20)
Atopy test positive	36/89 (40.4%)	68/77 (88.3%)	178/239 (74.5%)	46/78 (58.9%)	NA	NA
Participants prescribed OCS	NA	NA	160/310 (52%)	50/108 (46%)	85/225 (37.8%)	28/80 (32.9%)
Prescribed OCS dose (mg prednisolone eq.)	NA	NA	12 (9-20)	16 (10-21)	15 (9-29)	16 (9-29)
Prednisolone detected in urine (n)	NA	NA	101/310 (32.6%)	31/108 (28.7%)	61/225 (27.1%)	24/80 (28.2%)

Confirmed OCS users[2]	NA	NA	66/310 (21.3%)	25/108 (23.1%)	29/225 (12.9%)	12/80 (15%)
Prescribed OCS dose (mg prednisolone eq.) in confirmed OCS users	NA	NA	10 (7.5-15)	10 (10-20)	10 (5-15)	10(10-20)
Confirmed OCS non-users[3]	NA	NA	123/310 (39.7%)	49/108 (45.3%)	100/225 (44.4%)	40/80 (50%)
Theophylline users[4]	NA	NA	54/310 (17.4%)	22/108 (20.3%)	39/225 (17.3%)	16/80 (20%)
Theophylline non-users[5]	NA	NA	245/310 (79%)	85/108 (78.7%)	178/225 (79.1%)	64/80 (80%)
Omalizumab users	NA	NA	39/310 (12.5%)	13/108 (12.0%)	33/225 (14.7%)	10/80 (12.5%)
Serum-IgE matched omalizumab non-users[6]	NA	NA	71/310 (22.9%)	26/108 (24.1%)	54/225 (24.0%)	26/80 (32.5%)
Anticholinergic users[4]	NA	NA	68/310 (21.9%)	31/108 (28.7%)	54/225 (24.0%)	23/80 (28.8%)
Anticholinergic non-users[5]	NA	NA	230/310 (74.2%)	75/108 (69.4%)	152/225 (67.6%)	51/80 (63.8%)
Leukotriene modifier users[4]	NA	NA	131/310 (42.3%)	42/108 (38.9%)	87/225 (38.7%)	28/80 (35%)
Leukotriene modifier non-users[5]	NA	NA	169/310 (54.5%)	62/108 (57.4%)	117/225 (52.0%)	48/80 (60.0%)

Number (%), median (IQR), n/N (%)

NA, not applicable; OCS, oral corticosteroids

[1]Non-smoking status was defined as being never smokers or non-smokers for at least the last 12 months with less than 5 pack-year smoking history

[2]Reported at least daily use of OCS and positive detection of the presence of prednisolone or prednisone, methylprednisolone, 16α-OH-prednisolone, 20β-dihydroprednisolone, or desacetyl deflazacort in urine

[3]Reported no prior use of OCS, and OCS metabolites were not detected in urine

[4]Reported at least daily use

[5]Reported no prior use

[6]Serum-IgE matched individuals with no prior omalizumab use

Table 2. Metabolites associated with oral corticosteroid (OCS)*

Metabolite	Cluster[†]	SAns (n=123)[‡]	SAns + OCS (n=66)	p-value[§]	FDR
Cystathionine	A	0.87 (0.71,1.14)	1.1 (0.85,1.53)	0.005	0.003
Histidine	A	0.87 (0.73,0.98)	0.77 (0.61,0.85)	0.005	0.003
Isoleucine	A	1.1 (0.92,1.2)	0.92 (0.77,1.06)	0.029	0.010
5-Aminolevulinic acid	B	0.91 (0.76,1.12)	0.76 (0.58,0.92)	0.046	0.015
Kynurenic acid	B	0.89 (0.78,1.04)	0.82 (0.73,0.95)	0.047	0.014
Uracil	B	0.86 (0.73,1.01)	0.66 (0.52,0.78)	2.16E-4	0.001
5-Hydroxyindoleacetic acid	D	1.06 (0.96,1.19)	1.19 (1.04,1.34)	0.022	0.008
Aspartic acid	D	1.17 (0.98,1.35)	0.86 (0.73,1.07)	0.001	0.001
Glutamic acid[¶]	D	1.16 (1.04,1.37)	1.04 (0.90,1.20)	0.058	0.015
N-Acetylputrescine	D	1.06 (0.94,1.25)	1.24 (1.04,1.42)	0.035	0.012
N-Methyl-D-aspartic acid	D	0.92 (0.82,1)	1.16 (1.05,1.3)	7.52E-5	0.001
S-Adenosylhomocysteine	D	1 (0.83,1.16)	1.15 (1.04,1.38)	0.004	0.003
Serotonin	D	1.23 (1.06,1.44)	1.41 (1.17,1.83)	0.017	0.007
Methylthioadenosine	E	1.25 (1.07,1.65)	0.9 (0.72,1.26)	0.003	0.003
Xanthine	E	1.16 (0.97,1.39)	0.96 (0.69,1.18)	0.008	0.004
2-Furoylglycine	G	0.68 (0.47,0.9)	2.05 (1.24,3.15)	0.003	0.003
4-Pyridoxic acid	G	0.94 (0.84,1.05)	1.06 (0.88,1.36)	0.048	0.014
Allantoin	G	1.02 (0.84,1.26)	1.17 (0.95,1.47)	0.019	0.008
Aminovaleric acid	G	1.19 (0.71,1.78)	0.83 (0.44,1.21)	0.014	0.006
Glucosamine	G	0.87 (0.77,1.06)	1.18 (0.97,1.43)	0.003	0.003
Maltose	G	1.09 (0.91,1.49)	1.84 (1.19,2.86)	0.003	0.003
Methylhippuric acid	G	0.89 (0.71,1.16)	1.18 (0.94,1.49)	0.014	0.006
Sucrose	G	1.13 (0.83,1.51)	1.78 (1.34,2.35)	2.35E-04	0.001
Xylose	G	1 (0.82,1.16)	1.44 (1.01,2.04)	0.002	0.003

*All fold change estimates are in comparison to healthy participants
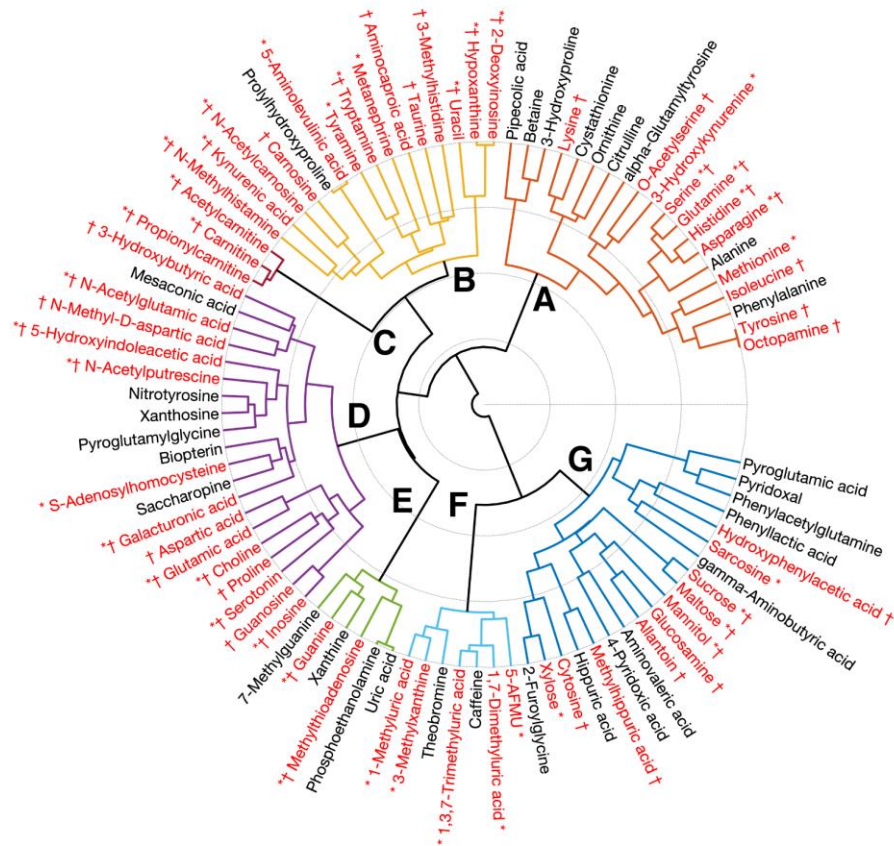[†]Cluster assignment as shown in Figure 1
[‡]SAns=non-smoking severe asthmatics
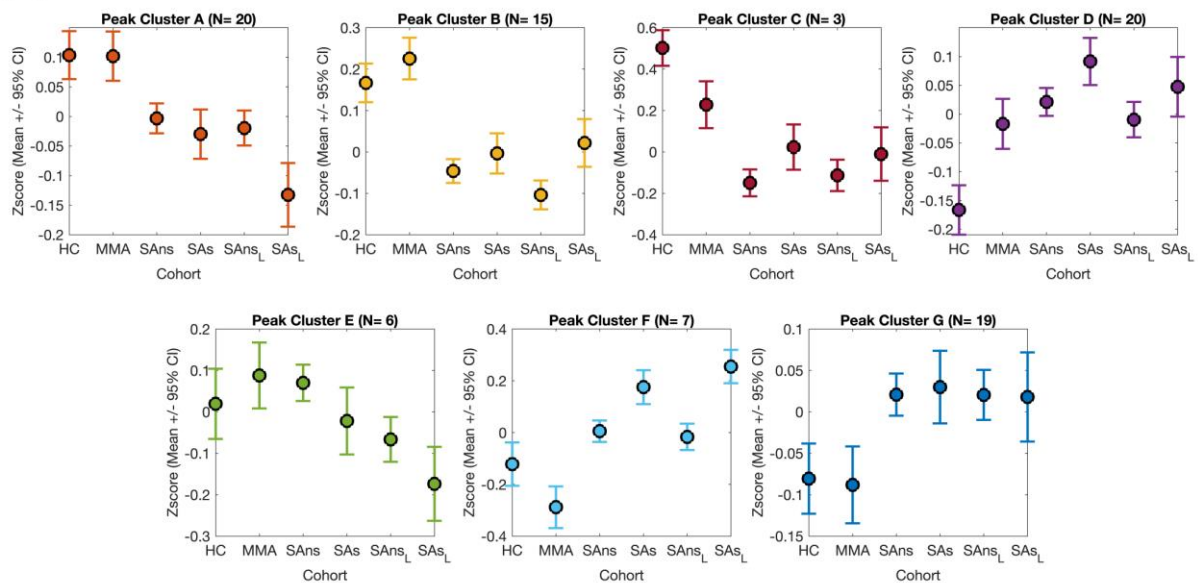[§]Wilcoxon Rank-Sum test between OCS-treated and non-treated groups
[¶]Glutamic acid was included due to its high magnitude of effect on the corresponding multivariate PC-CVA model (Figure 2)

Figure Captions

(A)

(B)

Figure 1. Hierarchical cluster analysis (HCA) of metabolite abundances. HCA was performed using multivariate Spearman correlation distance metric and Ward's group linkage. **(A)** Resulting metabolite clusters are presented as a polar dendrogram (differentially coloured and labelled as A-G). Black text, metabolite not significant in
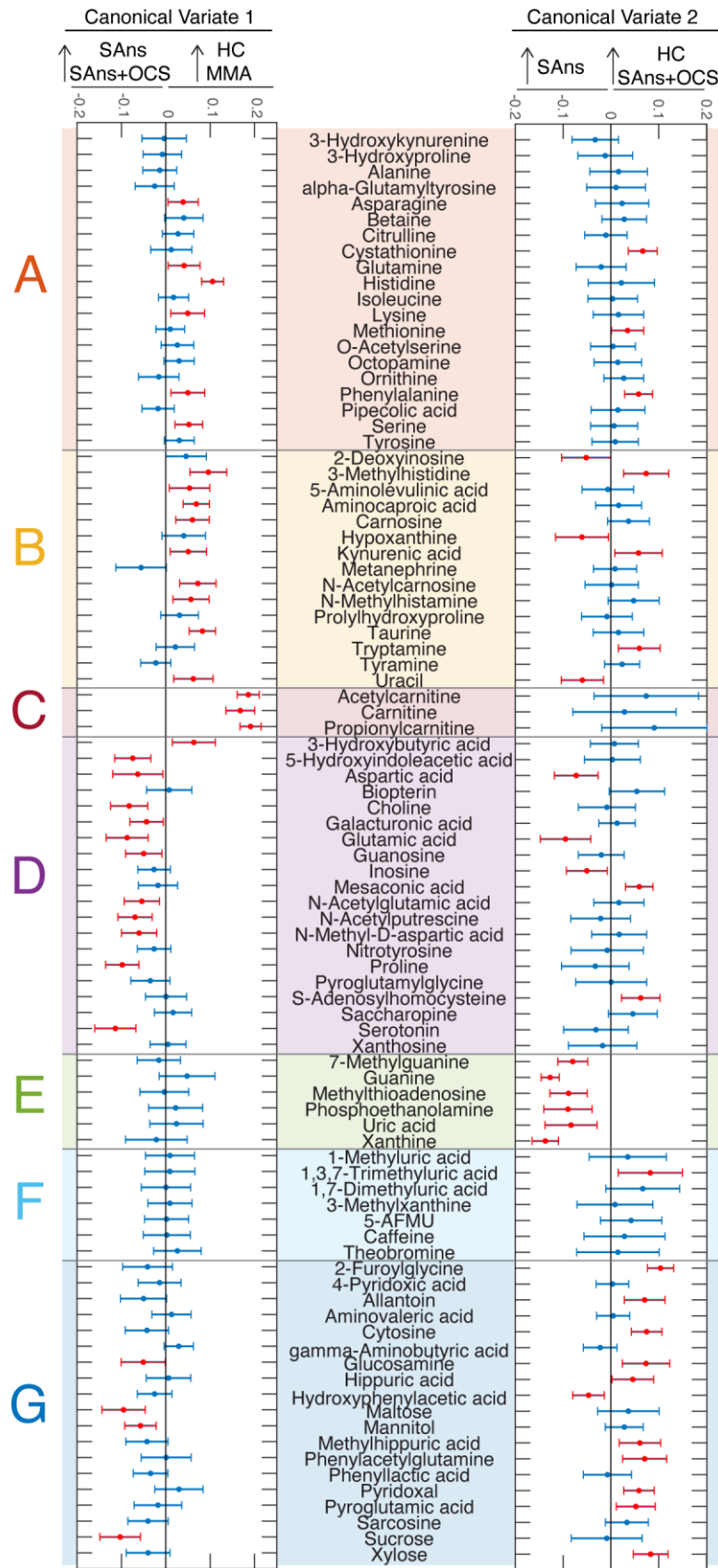
either univariate or multivariate analysis; red text, metabolite significant in univariate and/or multivariate analysis. *, p<0.05 univariate analysis; †, p<0.05, Canonical Variate 1 (CV1, see **Figure E1C**). **(B)** The mean of log-transformed and z-scaled data of the resulting clusters plotted against the clinical groups. HC, healthy control participants; MMA, mild-to-moderate asthma; SAns, severe asthma non-smokers; SAs, severe asthma ex/smokers; L, longitudinal data.
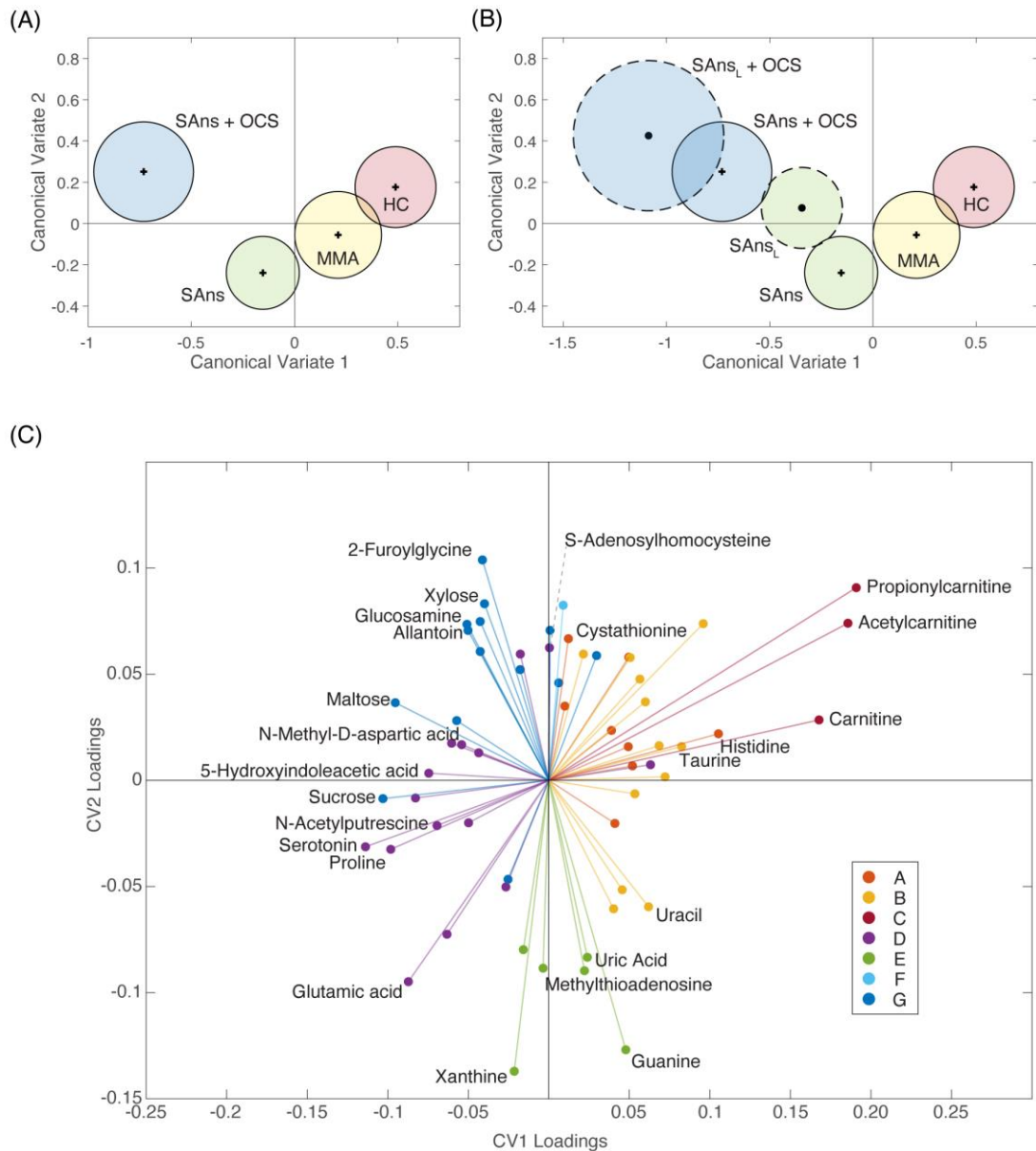
Figure 2. Principal Components – Canonical Variate Analysis (PC-CVA) with non-smoking severe asthmatics stratified by oral corticosteroid (OCS) use. Cross validation showed that 5 Principal Components were the optimal number to use in the CVA model (Figure E2). **(A)** Scores plot of baseline data, labelled by clinical class. Red, healthy controls; yellow, mild-to-moderate asthma (MMA); green, severe asthma non-smokers (SAns); blue, severe asthma non-smokers taking OCS treatment (SAns + OCS). **(B)** Longitudinal data for severe asthma groups projected into the

baseline model. L, longitudinal data. **+**, mean of each baseline group; •, mean of each longitudinal group; solid circles, 95% confidence intervals of the mean of baseline groups; dashed circles, 95% confidence interval of the mean of longitudinal groups. **(C)** Loadings plot displaying metabolites that significantly ($p<0.05$) contribute to the model. Metabolite position displays the magnitude and direction of affect in CV1 (x-axis) and CV2 (y-axis). The quadrant positions of metabolites are related to those of the clinical groups in the scores plots. In other words, metabolites are most abundant in the clinical groups with which they share a quadrant. Metabolites are colour-coded based on corresponding cluster as identified in **Figure 1** and according to the figure legend.

Canonical Variate 1

↑ SAns / SAns+OCS   ↑ HC / MMA

-0.2 -0.1 0 0.1 0.2

Canonical Variate 2

↑ SAns   ↑ HC / SAns+OCS

-0.2 -0.1 0 0.1 0.2

A
3-Hydroxykynurenine
3-Hydroxyproline
Alanine
alpha-Glutamyltyrosine
Asparagine
Betaine
Citrulline
Cystathionine
Glutamine
Histidine
Isoleucine
Lysine
Methionine
O-Acetylserine
Octopamine
Ornithine
Phenylalanine
Pipecolic acid
Serine
Tyrosine

B
2-Deoxyinosine
3-Methylhistidine
5-Aminolevulinic acid
Aminocaproic acid
Carnosine
Hypoxanthine
Kynurenic acid
Metanephrine
N-Acetylcarnosine
N-Methylhistamine
Prolylhydroxyproline
Taurine
Tryptamine
Tyramine
Uracil

C
Acetylcarnitine
Carnitine
Propionylcarnitine

D
3-Hydroxybutyric acid
5-Hydroxyindoleacetic acid
Aspartic acid
Biopterin
Choline
Galacturonic acid
Glutamic acid
Guanosine
Inosine
Mesaconic acid
N-Acetylglutamic acid
N-Acetylputrescine
N-Methyl-D-aspartic acid
Nitrotyrosine
Proline
Pyroglutamylglycine
S-Adenosylhomocysteine
Saccharopine
Serotonin
Xanthosine

E
7-Methylguanine
Guanine
Methylthioadenosine
Phosphoethanolamine
Uric acid
Xanthine

F
1-Methyluric acid
1,3,7-Trimethyluric acid
1,7-Dimethyluric acid
3-Methylxanthine
5-AFMU
Caffeine
Theobromine

G
2-Furoylglycine
4-Pyridoxic acid
Allantoin
Aminovaleric acid
Cytosine
gamma-Aminobutyric acid
Glucosamine
Hippuric acid
Hydroxyphenylacetic acid
Maltose
Mannitol
Methylhippuric acid
Phenylacetylglutamine
Phenyllactic acid
Pyridoxal
Pyroglutamic acid
Sarcosine
Sucrose
Xylose

Figure 3. Individual Canonical Variate (CV) loadings for the PC-CVA with non-smoking severe asthmatics stratified by oral corticosteroid (OCS) use. Loadings plots for Canonical Variate 1 (CV1, left panel) and CV2 (right panel) are shown. Clinical group labels at the top of each panel reflect the group position along the CV axis, as described by the model; clinical groups were not combined for this analysis. Red, metabolites that significantly ($p < 0.05$) contribute to separation in the CV based on 500 iterations of bootstrap resampling / remodelling; blue, metabolites that do not significantly contribute to the separation in the CV. Metabolites are ordered and colour-coded by cluster **(Figure 1)**. The cluster label is presented on the left side of the figure.

(A)
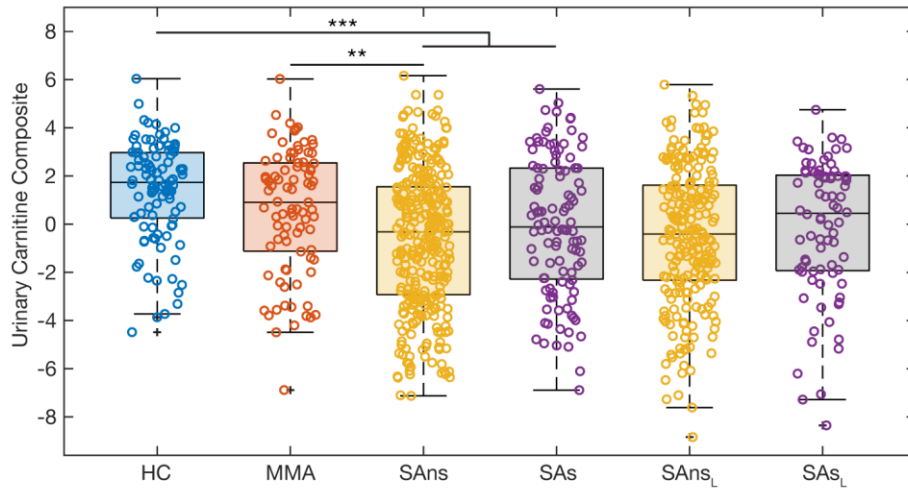
(B)
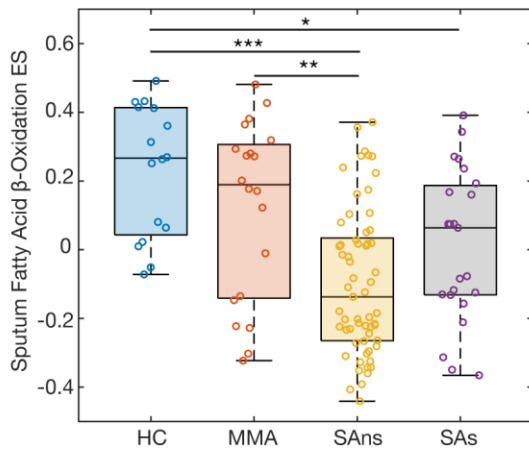
(C)
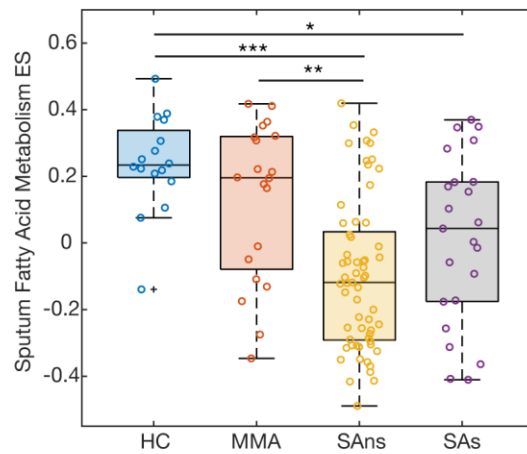
(D)
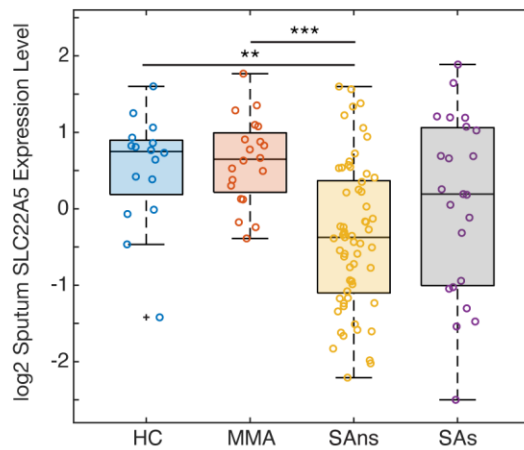
(E)
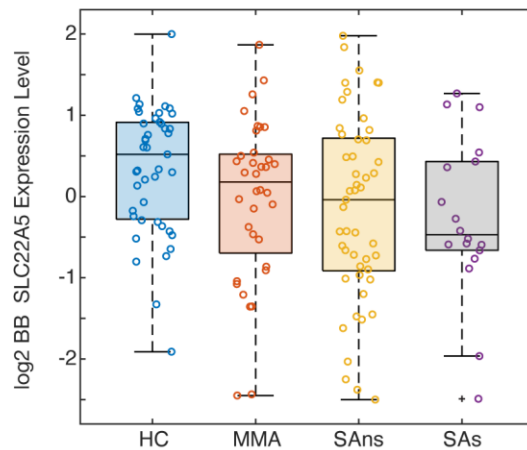
Figure 4. Molecular signatures of carnitine metabolism. Scatter-overlaid boxplots stratified by clinical class. **(A)** Urinary carnitine composite variable. Relative abundances of carnitine, acetylcarnitine and propionylcarnitine were log-transformed, z-scaled, and summed ($p=4\times10^{-9}$). **(B)** Sputum fatty acid β-oxidation gene set variance analysis (GSVA) enrichment score (ES) ($p=8.02\times10^{-6}$). **(C)** Sputum fatty acid metabolism GSVA ES ($p=6.29\times10^{-6}$). **(D)** Sputum SLC22A5 expression levels ($p=5.69\times10^{-5}$). **(E)** Bronchial brushings (BB) SLC22A5 expression levels ($p=0.0583$). Open circles, observations; box, median and interquartile range (IQR) of the data; whiskers, range of data up to 1.5 times of IQR above Q3 or below Q1; +, outliers. Kruskal-wallis p-values are reported here, with posthoc pairwise comparisons shown on the figure. *, $p<0.05$; **, $p<0.01$; ***, $p<0.001$. HC, healthy control participants; MMA, mild-to-moderate asthma; SAns, severe asthma non-smokers; SAs, severe asthma ex/smokers; L, longitudinal data.
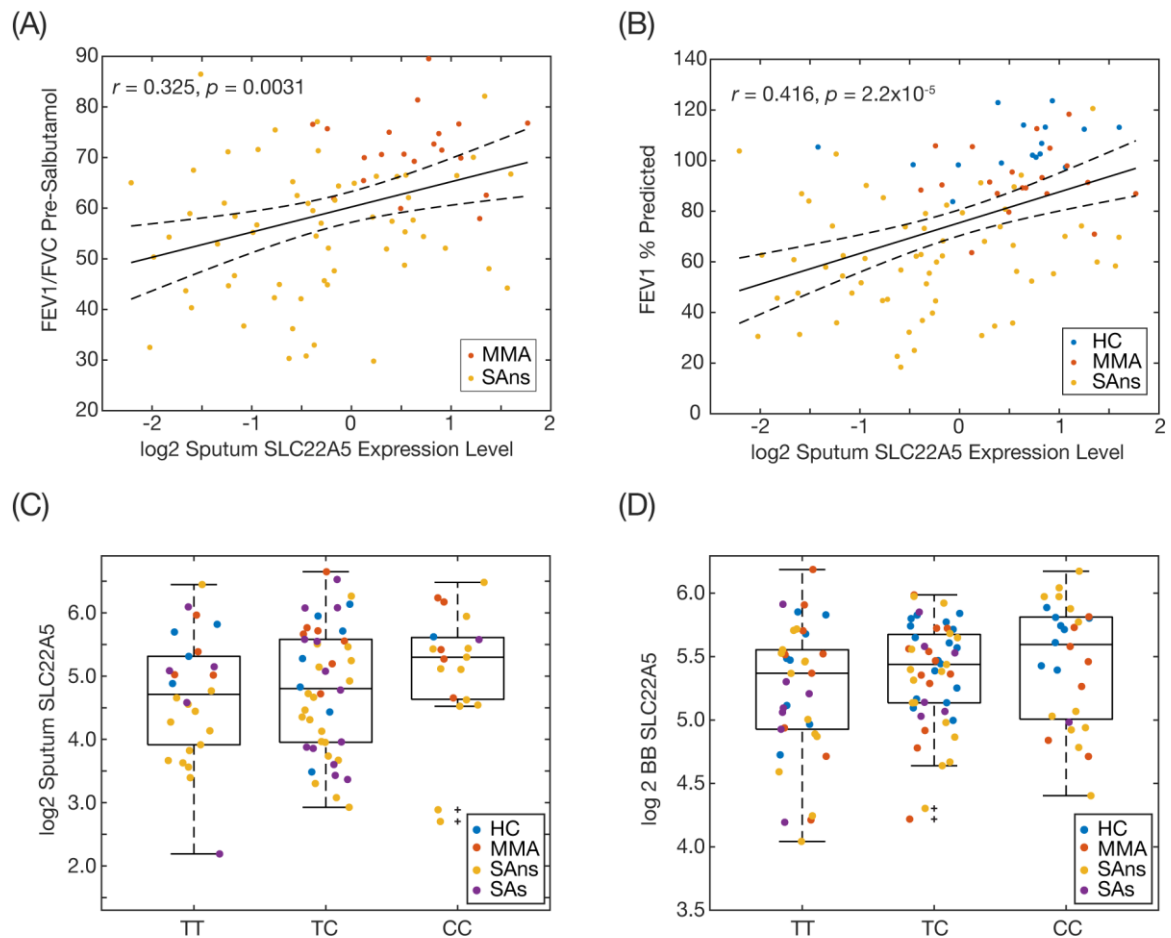
Figure 5. Relationship of SLC22A5 gene expression levels with lung function and genotype. (A) Correlation between FEV_1/FVC ratio pre-salbutamol and sputum SLC22A5 gene expression levels. **(B)** Correlation between $FEV_1\%$ predicted and sputum SLC22A5 gene expression levels. All assumptions for parametric analysis were verified, thus Pearson correlation was used. Dots, observations; solid line, regression; dashed lines, 95% confidence intervals of the regression. A weak linear correlation was also observed between the urinary carnitine composite and $FEV_1\%$ predicted (r=0.15, p=1.43×10^{-4}), but not FEV_1/FVC ratio pre-salbutamol (p=0.90). **(C)** Relationship between sputum SLC22A5 gene expression levels and genotype (effect allele C: beta=0.234, SD=0.148, p=0.119; n=91) **(D)** Relationship between bronchial brushing SLC22A5 gene expression levels and genotype (effect allele C: beta=0.138,

SD=0.057, p=0.028; n=118). The p-value of the effect size/coefficient of genotype in the regression model was used to test if the SNP was significantly associated with the gene expression. Open circles, observations; box, median and interquartile range (IQR) of the data; whiskers, range of data up to 1.5 times of IQR above Q3 or below Q1; +, outliers. BB, bronchial brushings; HC, healthy control participants; MMA, mild-to-moderate asthma; SAns, severe asthma non-smokers; SAs, severe asthma ex/smokers.
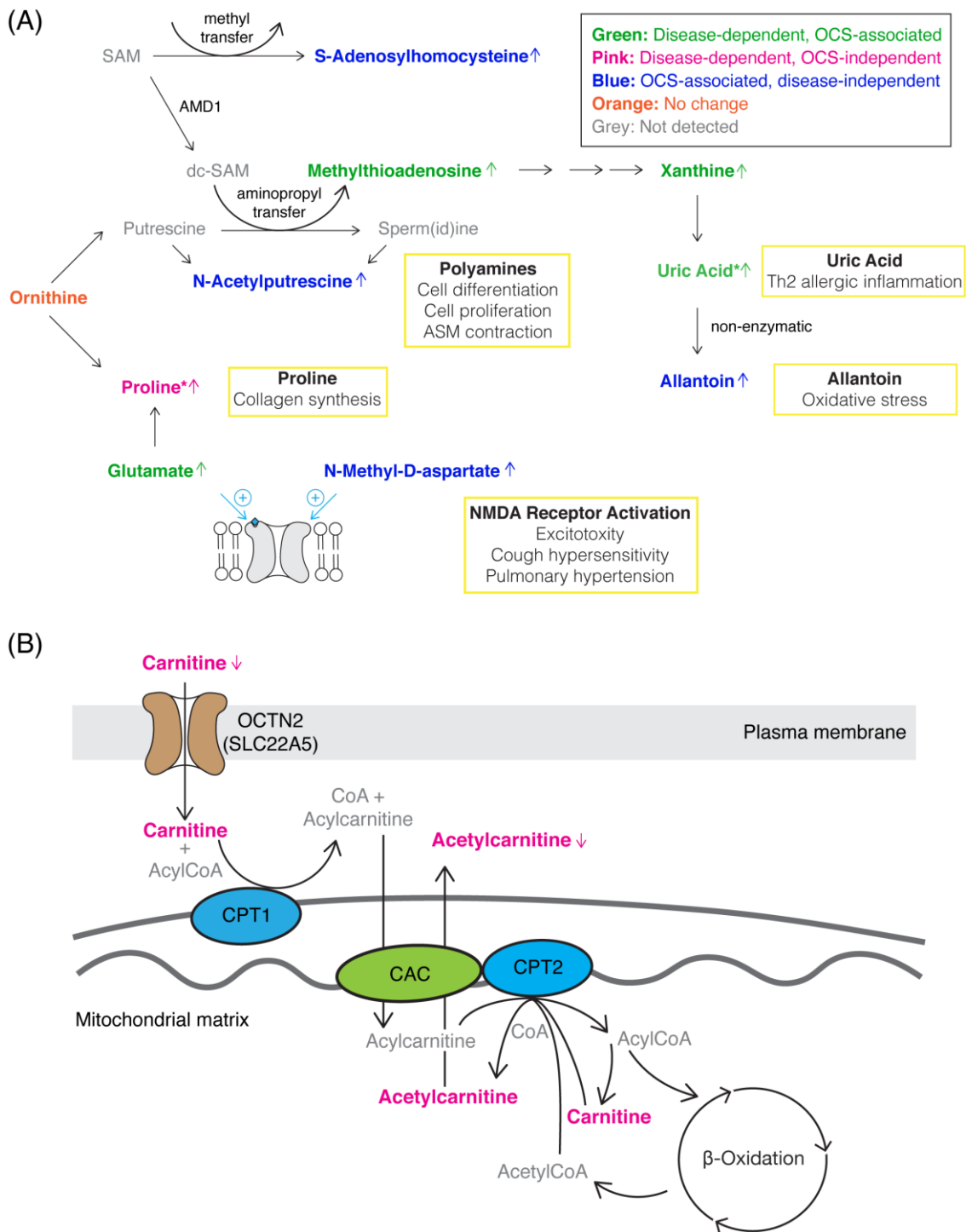
Figure 6. Biochemical pathways underlying severe asthma observed in the current study. (A) Metabolism associated with OCS use. (**B**) Carnitine metabolism. Green, OCS-associated alteration in severe asthma; pink, OCS-independent alteration in asthma; blue, OCS-associated, disease-independent alteration; orange,

no change observed; grey, metabolites not detected in the current study; black, notes on metabolic reactions; yellow boxes, known pathogenic mechanisms of asthma. Arrows indicate direction of change. Abbreviations: AMD1, adenosylmethionine decarboxylase; ASM, airway smoother muscle; CAC, carnitine-acylcarnitine carrier; CPT, carnitine palmitoyltransferase; dcSAM, decarboxylated SAM; OCTN, organic cation transporter novel; SAM, S-adenosylmethionine. *, shift observed via multivariate analysis only.

Urinary metabotype of severe asthma evidences decreased carnitine metabolism independent of oral corticosteroid treatment in the U-BIOPRED Study

Stacey N. Reinke[1,2,†], Shama Naz[1,†], Romanas Chaleckis[1,3], Hector Gallart-Ayala[1], Johan Kolmert[1,4], Nazanin Z. Kermani[5], Angelica Tiotiu[5,6], David I. Broadhurst[2], Anders Lundqvist[7], Henric Olsson[8] Marika Ström[9,10], Åsa M. Wheelock[9,10], Cristina Gómez[1,4], Magnus Ericsson[11], Ana R. Sousa[12], John H. Riley[12], Stewart Bates[12], James Scholfield[13], Matthew Loza[14], Frédéric Baribaud[14], Per S. Bakke[15], Massimo Caruso[16], Pascal Chanez[17], Stephen J. Fowler[18], Thomas Geiser[19], Peter Howarth[13], Ildikó Horváth[20], Norbert Krug[21], Paolo Montuschi[22], Annelie Behndig[23], Florian Singer[24], Jacek Musial[25], Dominick E. Shaw[26], Barbro Dahlén[10], Sile Hu[27], Jessica Lasky-Su[28], Peter J. Sterk[29], Kian Fan Chung[5], Ratko Djukanovic[13], Sven-Erik Dahlén[4,27], Ian M. Adcock[5], *Craig E. Wheelock[1,3,10], on behalf of the U-BIOPRED Study Group#

Affiliations:
1) Division of Physiological Chemistry 2, Department of Medical Biochemistry and Biophysics, Karolinska Institute, Stockholm, Sweden.
2) Centre for Integrative Metabolomics & Computational Biology, School of Science, Edith Cowan University, Perth, Australia
3) Gunma Initiative for Advanced Research (GIAR), Gunma University, Maebashi, Japan
4) The Institute of Environmental Medicine, Karolinska Institutet, Stockholm, Sweden
5) National Heart and Lung Institute, Imperial College, London, U.K.
6) Department of Pulmonology, University Hospital of Nancy, Nancy, France
7) DMPK, Research and Early Development, Respiratory & Immunology, BioPharmaceuticals R&D, AstraZeneca, Gothenburg, Sweden
8) Translational Science and Experimental Medicine, Research and Early Development, Respiratory & Immunology, BioPharmaceuticals R&D, AstraZeneca, Gothenburg, Sweden
9) Respiratory Medicine Unit, K2 Department of Medicine Solna and Center for Molecular Medicine, Karolinska Institutet, Stockholm, Sweden
10) Department of Respiratory Medicine and Allergy, Karolinska University Hospital, Stockholm, Sweden
11) Department of Clinical Pharmacology, Huddinge Campus, Karolinska Institutet and Karolinska University Hospital, Stockholm, Sweden
12) Glaxo Smith Kline, London, U.K.
13) Faculty of Medicine, Southampton University and NIHR Southampton Respiratory Biomedical Research Center, University Hospital Southampton, Southampton, U.K.
14) Janssen Research and Development, High Wycombe, U.K.
15) Institute of Medicine, University of Bergen, Bergen, Norway
16) Department of Biomedical and Biotechnological Sciences and Department of Clinical and Experimental Medicine, University of Catania, Catania, Italy
17) Assistance Publique des Hôpitaux de Marseille, Clinique des Bronches, Allergies et Sommeil, Aix Marseille Université, Marseille, France
18) Division of Infection, Immunity and Respiratory Medicine, School of Biological Sciences, Faculty of Biology, Medicine and Health, University of Manchester, and

Manchester Academic Health Science Centre and NIHR Biomedical Research Centre, Manchester University Hospitals NHS Foundation Trust, Manchester, U.K.

19) Department of Pulmonary Medicine, University Hospital, University of Bern, Switzerland
20) Department of Pulmonology, Semmelweis University, Budapest, Hungary
21) Fraunhofer Institute for Toxicology and Experimental Medicine, Hannover, Germany
22) Pharmacology, Catholic University of the Sacred Heart, Rome, Italy
23) Department of Public Health and Clinical Medicine, Section of Medicine, Umeå University, Umeå, Sweden
24) Division of Paediatric Respiratory Medicine and Allergology, Department of Paediatrics, Inselspital, Bern University Hospital, University of Bern, Switzerland
25) Dept of Medicine, Jagiellonian University Medical College, Krakow, Poland
26) Nottingham NIHR Biomedical Research Centre, University of Nottingham, U.K.
27) Data Science Institute, Imperial College, London, U.K.
28) Channing Division of Network Medicine, Brigham and Women's Hospital and Harvard Medical School, Boston, MA, USA
29) Department of Respiratory Medicine, Amsterdam UMC, University of Amsterdam, Amsterdam, The Netherlands

[†]equal contribution

*corresponding author
Craig E Wheelock
Division of Physiological Chemistry 2
Department of Medical Biochemistry and Biophysics
Karolinska Institutet
Solnavägen 9, Biomedicum Quartier 9A
171 77 Stockholm, Sweden
Telephone: +46-852487630
Email: craig.wheelock@ki.se

Methods

Study Subjects and Design

A total of 605 participants from the pan-European U-BIOPRED study (Unbiased Biomarkers for the Prediction of Respiratory Disease outcomes) were included (**Table 1**). Participants from 15 clinical sites were included and asthma was classified according to international guidelines on severe asthma with the following groups; healthy controls (HC, n=100), mild-to-moderate asthmatics (MMA, n=87), non-smoking severe asthmatics (SAns, n=310), and smoking/ex-smoking severe asthmatics (SAs, n=108) [1]. All participants provided a urine sample within 28 days of initial screening (baseline visit); an additional urine sample was provided by 225 SAns and 80 SAs participants at a longitudinal follow-up visit 12-18 months later. A brief overview of baseline and longitudinal clinical and demographic characteristics is shown in (Table 1), with a more detailed baseline description found elsewhere [1]. Ethics approval was obtained from each participating clinical institution and all participants provided written informed consent. U-BIOPRED adhered to standards outlined by the International Conference on Harmonisation and Good Clinical Practice and is registered on ClinicalTrials.gov (identifier: NCT01976767).

Medication use

All MMA subjects were on ≤500 μg inhaled fluticasone equivalents/day (ICS), while all SA subjects received ≥1000 μg fluticasone equivalents/day. Of the severe asthmatics, 50% were prescribed oral corticosteroids (OCS), 18% were prescribed theophylline, and 12% were treated with anti-IgE therapy (*i.e.,* omalizumab). Regular use of non-steroidal anti-inflammatory drugs (NSAIDs) was part of the exclusion criteria. Reliever medication, such as short/long acting β_2 agonists (SABA/LABA) or combination

therapy was used by all asthmatic subjects. In sub-groups of asthmatics anticholinergics and chromoglycate was used among others, of which use was reported to be 18% and 2%, respectively.

Participant stratification by asthma treatment

Severe asthmatic non-smoker participants were stratified by treatment. OCS stratification was previously described [2]. Participants reporting at least daily use of OCS and had detectable OCS metabolites in their urine were classified as confirmed OCS users. Participants reporting never or previous use of OCS and did not have detectable OCS metabolites in their urine were classified as confirmed non-users of OCS. Theophylline stratifications were based on participant reported use. Participants reporting at least daily use of theophylline were considered users; those reporting no prior use were considered non-users. Omalizumab stratification was based on medical records of administration. Serum-IgE matched individuals with no prior use were considered non-users using a 2:1 nested case-control design as described by Kolmert et al. [2].

Metabolomics analysis

Metabolomics data were acquired by liquid chromatography – high resolution mass spectrometry (LC-HRMS) using previously described methods [3]. The analytical sequence (injection order) was randomised by clinical group, sex, age, BMI, collection site, and ethnicity to avoid analytical bias [4]; matching baseline and longitudinal samples were placed together in the analytical sequence in alternating order. To normalise for urine concentration and to reduce matrix effects [5], the specific gravity (SG) was measured. Prior to analysis, batches of 100 x 5 ml urine samples were

thawed at 4°C, then centrifuged for 5 minutes at 250 rcf to pellet any precipitate. For each sample, 100 μL was used to measure SG on a refractometer (Atago UG-a), 100 μL was used to create a pooled quality control (QC) sample and 5 x 500 μl aliquots were prepared and returned to -80°C. A pooled QC was made for each daily batch. After the final batch, all daily pooled QC samples were thawed to prepare a final pooled QC; the SG was measured for this sample and sub-aliquots were prepared for each analytical batch. In total, samples were analysed in 17 batches with pooled quality control (QC) samples analysed after every 5th sample to monitor analytical drift and measure precision [6]. On the day of analysis, urine samples were diluted with LC-MS grade water (Sigma-Aldrich, St. Louis, MO, USA) to the lowest SG (1.00x) measurements of the sample set and prepared as described [3]. Metabolite extraction was then performed by adding 180 μL of LC-MS grade acetonitrile (Fisher Scientific, Loughborough, UK) containing internal standards to 20 μL of SG-diluted urine. Samples were vortexed briefly then centrifuged at 13,000 x g for 15 minutes at 4°C; 40 μL of the supernatant was transferred to an LC-MS vial containing an insert for analysis.

Data were acquired using a 1290 Infinity II ultra-high performance liquid chromatography system coupled to an Agilent 6550 iFunnel Q-TOF mass spectrometer (Agilent Technologies, Santa Clara, CA, USA). Metabolites were separated using hydrophilic interaction liquid chromatography (SeQuant ZIC-HILIC column 100 Å, 100 × 2.1 mm, 3.5 μm particle size) coupled to a 2.1 × 2 mm, 3.5 μm particle size guard column (Merck, Darmstadt, Germany) and an inline-filter. Mass spectral data were acquired in both electrospray ionisation (ESI) positive and negative modes. The mobile phases for ESI-positive ionization mode were water containing

0.1% formic acid (solvent A) and acetonitrile containing 0.1% formic acid (solvent B), and for ESI-negative ionization mode were 10 mM ammonium acetate pH 6.7 (solvent A) and acetonitrile (solvent B). The elution gradient was as follows: 1.5 min at 95% [B], 95 to 40% [B] in 12 min, maintained at 40% [B] for 2 min, then decreasing to 25% [B] at 14.2 min, maintained for 2.8 min, then returned to initial conditions over 1 min, and then the column was equilibrated at initial conditions for 7 min. The flow rate was 0.3 mL/min; injection volume was 2 µL, and the column oven was maintained at 25 °C

Data were acquired in a mass range of 40–1200 *m/z* using the following settings: sheath gas, N_2, 8 L/min; drying gas, N_2, 15 L/min; gas temperature, 250°C; nebulizer pressure, 35 psi; voltage, 3000 V; fragmentor voltage, 380 V. All data were acquired using all ions fragmentation (AIF) mode; this included three sequential experiments at three alternating collision energies (0 eV, 10 eV, and 30 eV). The data acquisition rate was 6 scans/s.

Peak deconvolution and metabolite identification were performed using Agilent TOF-Quant software (version B.07.00, Agilent Technologies) as described [3]. To ensure accurate metabolite identification, metabolites were matched against retention time, accurate mass, and MS/MS fragmentation patterns of 408 chemical reference standards in an in-house database. Metabolites were only included for statistical analysis if the accurate mass, retention time, and MS/MS fragmentation pattern matched to an authentic standard; thus, all metabolites reported have a Level 1 identification level as defined by the Metabolite Standards Initiative [7].

Systematic experimental within- and between-batch variation was corrected using the QC- Robust Spline Correction (QC-RSC) algorithm [8]. Metabolite abundances were then plotted against injection order and visually inspected to identify deconvolution problems; deconvolution was optimised and repeated as necessary. Following this procedure, the relative standard deviation of the pooled QC samples (QC_{RSD}) and the ratio of QC variance to sample variance (D-ratio) were calculated for each metabolite, aligning to community quality control best practice [6]. Quality assessment revealed high quality data as evidenced by an average relative standard deviation (RSD_{QC}) of 3.3%, an average D-Ratio of 8.2%, and 1.38% total missing values.

Tryptophan quantification

Tryptophan and 6 of its metabolites were quantified by reversed-phase liquid chromatography coupled to mass spectrometry (LC-MS/MS). Briefly, the urine samples were diluted 100 times in purified water and centrifuged (Eppendorf Centrifuge 5430 R) at 15,000 rcf for 10 min at 4°C. Part of the supernatant (200 µl) was transferred to a 96 deep well plate (Thermo Scientific 26052) and capped with a mat. Calibration curves were diluted in purified water and run together with the samples. Samples were analysed on an Agilent 1290 Infinity II system with multiwash function and an Agilent 6490 Ion Funnel triple quadrupole mass spectrometer. 5 µl of the sample extract was injected into a Zorbax Eclipse RRHD C18 column (50 × 2.1 mm, 1.8 µm particle size). A short gradient (0.5 ml/min flow rate, 40°C column oven) using 0.1 % formic acid in HPLC water (mobile phase A) (Milli-Q, Millipore) and 0.1 % formic acid in HPLC acetonitrile (mobile phase B) (Rathburn Chemicals) was applied. The gradient started at 2 % B increasing to 40 % B after 2 min and directly to a washing step at 95 % B for 0.6 minutes and then returned to initial conditions followed by an

0.8-minute column re-equilibration. Mass spectrometry data (MRM, multiple reaction monitoring) were acquired in positive electrospray ionization mode, using the transitions 225.09>109.9, 209.09>146.0, 205.1>188.1, 192.07>145.9, 190.05>144.0, 177.1>160.0 and 168.03>105.9 for 3-hydroxykynurenine, kyrunenine, tryptophan, 5-hydroxyindoleacetic acid, kynurenic acid, serotonin and quinolinic acid, respectively. Fragmentor voltage was set to 380 V and the Collision energies ranged from 10 to 18 V. In positive mode, the capillary voltage was 4.0 kV with a sheath gas temperature of 400°C and gas flow of 12 l/min. The Ion Funnel parameters were 200 and 110 for the high and low pressure radio frequencies. Data handling and quantification was performed using Agilent MassHunter B06.00 software. Samples were randomized across each batch to prevent potential confounding signal drift.

Genotyping

Sputum and bronchial brushing cis-eQTL summary statistic data were obtained in U-BIOPRED. The U-BIOPRED genotype data was imputed by IMPUTE2 [9] using 1000Genome phase 3 data [10] as the reference panel. The sputum eQTL analysis was performed on 91 U-BIOPRED participants that had both genetic and gene expression data in sputum available, and the bronchial brushing eQTL analysis was performed on 118 U-BIOPRED participants that had both genetic and gene expression data in bronchial brushings available. The eQTL analysis was performed with matrixEQTL in R [11] using age, sex and 10 principle components as covariates. The asthma GWAS summary statistics were also downloaded from a recent large scale GWAS study [12]. The number of cases and controls in the adult-onset GWAS were 26,582 and 327,253, respectively. The genome build used for both the eQTL and GWAS summary statistic was GRCh37. To determine if any of the SLC22A5 cis-eQTLs

overlapped with the asthma GWAS hits, a p-value threshold of 0.05 was applied for sputum and bronchial brushing eQTLs and genome-wide threshold of 5e-8 for GWAS SNPs. A lenient threshold was applied for the eQTL due to the fact that the eQTLs in sputum and bronchial brushing were underpowered due to the small sample size. We then subset the eQTLs with their asthma GWAS summary statistics also available, and aligned them to have the same effect allele with their GWAS summary statistics.

Statistical analysis

Missing values were imputed using the K-nearest neighbour (K=3) method, as is standard practice for metabolomics [13]. Metabolomics data, expressed as relative abundances, were not normally distributed (Lilliefors test); non-parametric univariate statistical tests were subsequently used. The null hypothesis (H_0), that the distribution of each metabolite was the same across outcomes, was tested using the Wilcoxon Rank-sum (2 outcomes) and Kruskal-Wallis test (more than 2 outcomes). The H_0, that baseline and longitudinal distributions were the same for each metabolite, was tested using the Wilcoxon signed-rank test. The Storey positive false discovery rate (FDR) [14] was calculated for all univariate analyses. Median fold-changes and confidence intervals were estimated using 500 iterations of bootstrap resampling [15] as previously reported [16]. Confounder correction was performed on the log urinary carnitine abundances using multiple linear regression, adjusting the clinical outcome for sex, age, and BMI. To provide robustness against heteroscedasticity, Huber's sandwich estimator for the regression coefficient standard errors was used [17]. Collection site-specific batch effects upon the observed metabotypes were evaluated and found to vary with metabolite.

To identify similarities between metabolites, hierarchical cluster analysis (HCA) was performed using a multivariate Spearman correlation distance metric and Ward's group linkage. The most similar metabolites form the lowest linkages in the resulting circular dendrogram; thus, emergent clusters represent similar trends. The mean of the log-transformed and z-scaled data of the resulting clusters were plotted against clinical groups to qualitatively visualise metabolite patterns across clinical groups. Principal Components – Canonical Variate Analysis (PC-CVA) was then performed, as previously described [16], to assess the multifactorial and correlated discrimination between clinical groups. Leave-one-out cross validation was used to determine the optimal number of PCs to be used in the model (**Figure E1**).

The targeted tryptophan data included 7 metabolites, including tryptophan and 6 downstream intermediates along 3 different pathways. Univariate analyses were performed using non-parametric tests (as described above). To visualise and assess clinical group differences across each pathway, mean data were presented in a bar graph and MANOVA was performed. Prior to MANOVA, data were normalised to tryptophan, log-transformed, and z-scaled.

In order to investigate the genetic impact of SLC22A5 on gene expression, we applied a linear regression framework to identify the cis-eQLTs associated with expression of SLC22A5. SNPs that were up to 1 MB (megabase) away from the TSS (transcription start site) of the gene were used in the association test. In the regression model, the genetic effect was assumed to be "additive", and standard linear regression was considered to model the genetic association with gene expression in SLC22A5:

$$E = \beta_0 + \beta_G G + \sum_{i=1}^{C} \beta_i C_i$$

Where E is log2-scaled gene expression, β_0 is the intercept term, G is the copies of effect allele, $C_{i=1,2...C}$ are the covariates including age, sex, asthma groups and 10 principal components extracted from the genetic related matrix. Our null hypothesis (H_0) was that effect size β_G =0, *i.e.,* there was no genetic association to the gene expression. A p-value of β_G less than a given threshold was then used to determine the significant genetic association. We used a p-value threshold 0.05 here without considering the multiple testing correction due to the smaller sample size, and we have therefore emphasised caution when interpreting the result.

Individual subject clinical and biochemical data were collected from the U-BIOPRED TranSMART platform (eTRIKS). All statistical analyses were performed using the MATLAB scripting language (Mathworks, Natick, MA, USA), R (3.4.4, CRAN Network), and STATA v14 (StataCorp LLC, College Station, TX, USA).

Results of the tryptophan pathway analyses

Targeted quantitative analyses were performed to further elucidate tryptophan metabolite alterations (**Figure E9, Table E10**). No changes were observed in tryptophan levels. Given the variability in the response, downstream metabolites were normalized to tryptophan levels on an intra-individual basis (**Figure E9**). Tryptophan metabolism was divided into 3 metabolic pathways: Monoamine oxidase (MAO), Indoleamine 2,3-dioxygenase (IDO), and Kynurenine 3-monooxygenase (KMO). Mild-to-moderate asthmatics had similar levels in all 3 pathways relative to healthy participants, while severe asthmatics were dysregulated relative to healthy participants. Smoking status exerted a minor effect upon the pathways. The observed patterns reached significance for the IDO and KMO pathways (p=0.01 and 0.03, respectively) and were replicated at the 12-to-18-month follow-up. Tryptophan metabolism was further probed at the mRNA level (**Table E11**). Of the detected transcripts from enzymes in these pathways, the majority exhibited no change in association with asthma status. However, IDO1 transcripts significantly increased in bronchial brushings, PBMCs, and sputum. The magnitude of the observed shifts for other transcripts was nominal and most likely not of importance.

**Discussion of the tryptophan pathway analyses**

There is significant interest in the potential role of tryptophan and its metabolites in multiple inflammatory diseases [18], including obstructive lung disease [19]. However, the literature is unclear in relation to asthma. We accordingly used the scale of the U-BIOPRED study to address this question. Tryptophan itself was unchanged in association with asthma severity or smoking status. However, the downstream metabolites were dysregulated with asthma severity and further perturbed by smoking

status (**Figure E9**). In the current study, the strongest observed changes were in the IDO pathway, which has previously been reported to be associated with allergic airway inflammation [19]. Of particular interest is that the transcript levels of IDO1 increased in bronchial brushings, sputum, and PBMCs, suggesting a systemic upregulation in this pathway that was reflected in the urinary metabotype. These profiles were generally stable at the 12-18 months longitudinal sampling. Serotonin was affected by smoking status as previously reported [20, 21], as well as OCS treatment. An intriguing hypothesis is that the tryptophan metabolites are produced by microbiota involved in the gut-lung axis [22], reflecting asthma-associated dysbiosis.

List of Supplementary Tables:

Table E1. Metabolite Information and Statistical Analysis by Cohort
Table E2. Baseline versus Longitudinal Analysis
Table E3. Effects of OCS on Metabolite Abundance
Table E4. Effects of Theophylline on Metabolite Abundance
Table E5. Effects of Omalizumab on Metabolite Abundance
Table E6. Effects of Anticholinergics on Metabolite Abundance
Table E7. Effects of Leukotriene Modifiers on Metabolite Abundance
Table E8. Summary of All Metabolites Significantly Affected by Therapeutics or Smoking in the SAns Group
Table E9. Confounder Correction on log(Urinary Carnitine Abundane)
Table E10. Analysis of Quantified Tryptophan Metabolites
Table E11. Tryptophan Metabolism Transcripts

Each supplementary table is presented in a separate sheet of the 'UBIOPRED_supplementary_tables.xlsx' file.
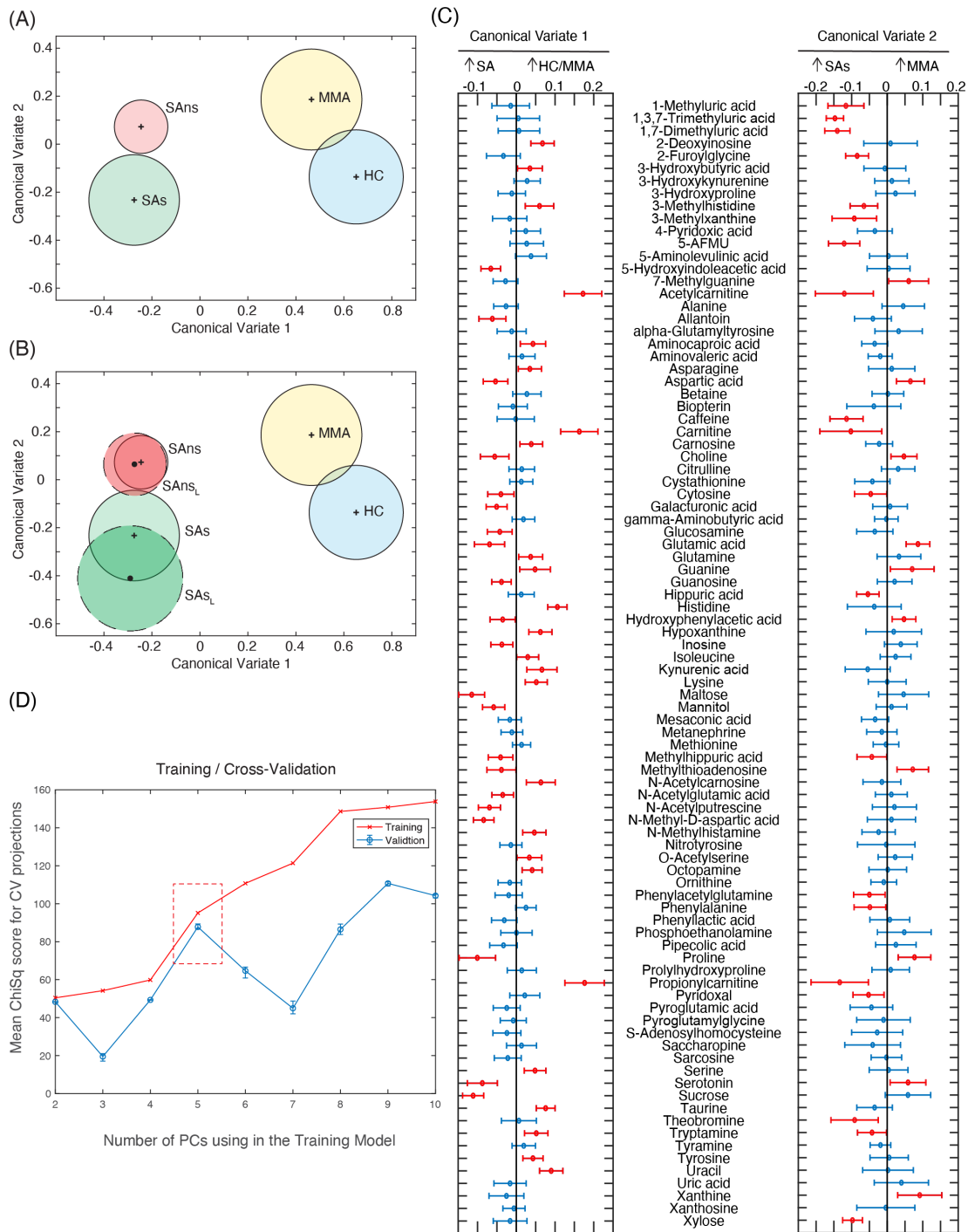
Figure E1. Principal Components – Canonical Variate Analysis (PC-CVA). (A) Scores plot of baseline data, labelled by clinical class. Blue, healthy controls; yellow, mild-to-moderate asthma (MMA); red, severe asthma non-smokers (SAns); green, severe asthma smokers (SAs). **(B)** Longitudinal data for severe asthma groups projected into the baseline model. $_B$, baseline data; $_L$, longitudinal data. +, mean of each baseline group; •, mean of each longitudinal group; solid circles, 95% confidence intervals of the mean of baseline groups; dashed circles, 95% confidence interval of the mean of longitudinal groups. **(C)** Loadings plots for Canonical Variate 1 (CV1, left panel) and CV2 (right panel). Red, metabolites that significantly (p<0.05) contribute to separation in the CV; blue, metabolites that do not significantly contribute to the separation in the CV. **(D)** Leave-one-out cross validation; 5 principal components were chosen as the number of optimal components to use in the model.
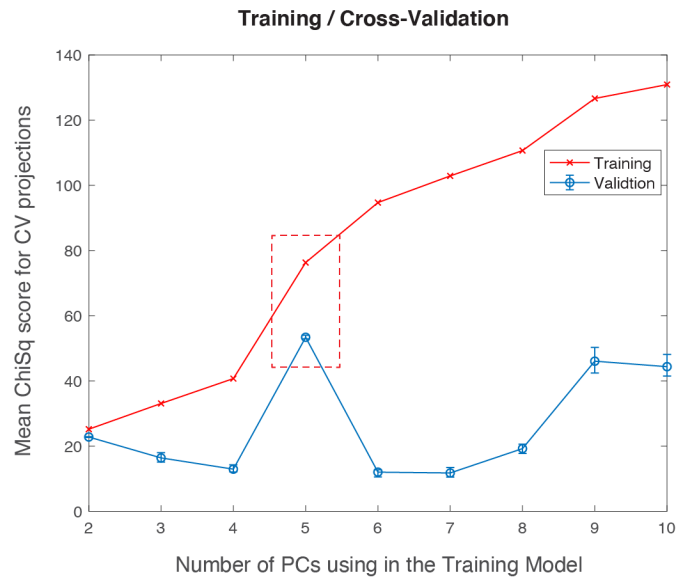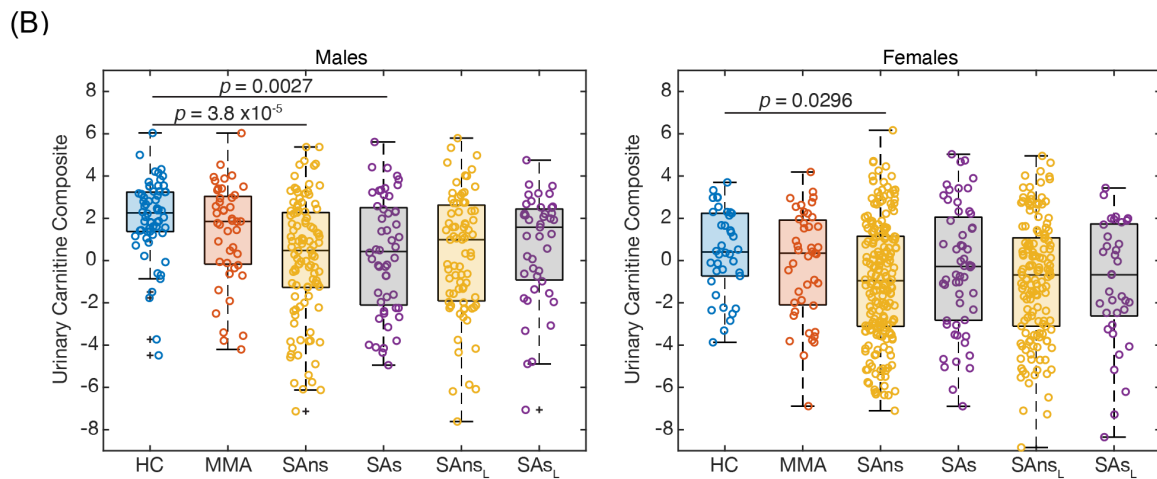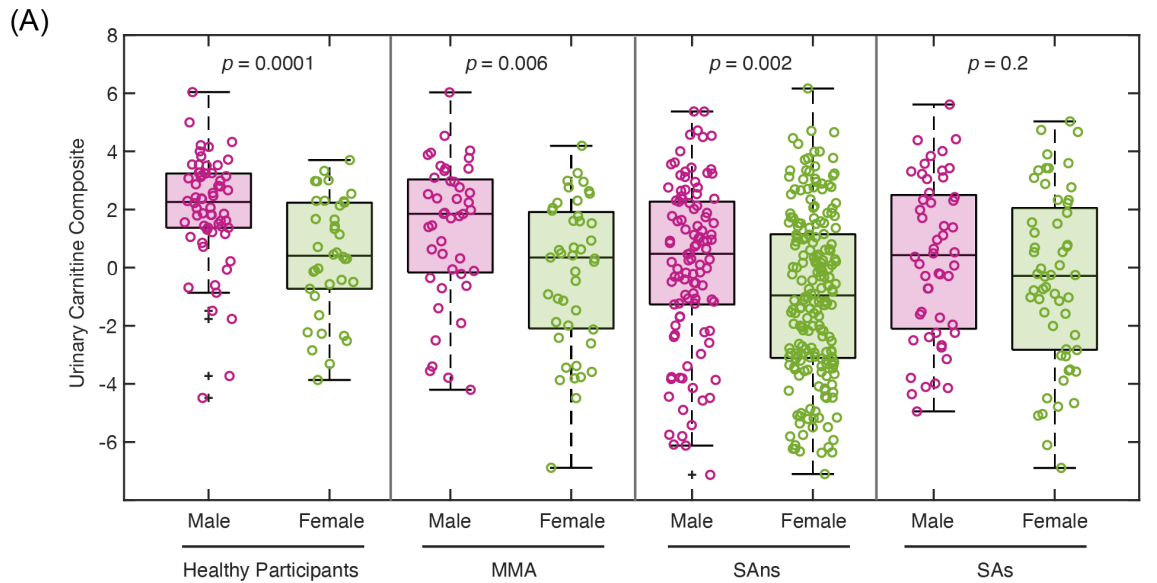
Figure E2. Cross Validation for the PC-CVA model presented in Figure 2. Leave-one-out cross validation was performed, identifying 5 principal components as the optimal number for the model.
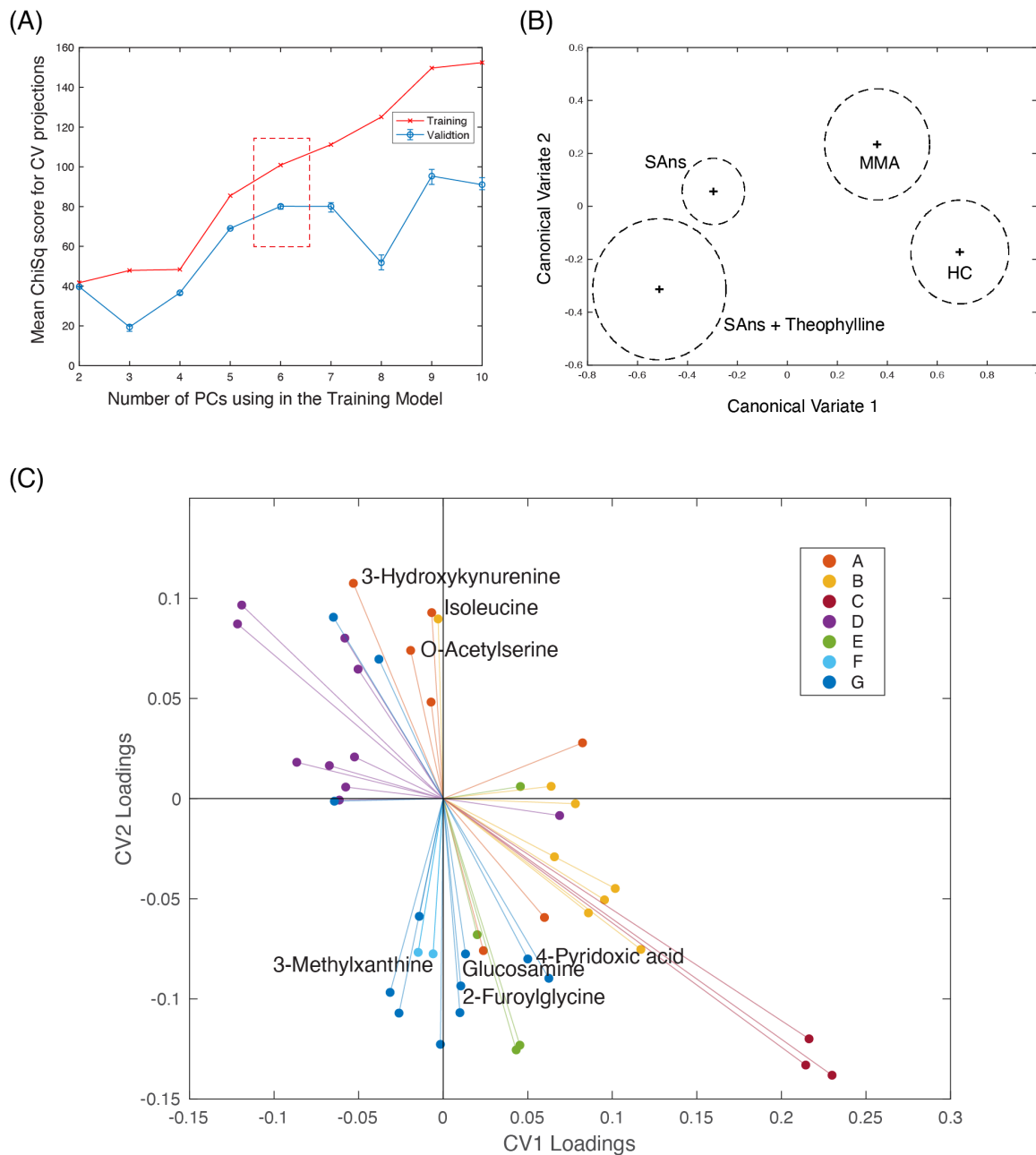
Figure E3. Principal Components – Canonical Variate Analysis (PC-CVA) with non-smoking severe asthmatics stratified by theophylline use. (A) Leave-one-out cross validation; 6 principal components were chosen as the number of optimal components to use in the model. **(B)** Scores plot labelled by outcome. HC, healthy control participants; MMA, mild-to-moderate asthmatics; SAns, severe asthma non-smokers; SAns + Theophylline, severe asthma non-smokers taking theophylline treatment. +, mean of each group; dashed circles, 95% confidence interval of the mean of each group. **(C)** Loadings plot displaying metabolites that significantly (p<0.05) contribute to the model. Metabolite position displays the magnitude and direction of affect in CV1 (x-axis) and CV2 (y-axis). The quadrant positions of metabolites are related to those of the clinical groups in the scores plots. In other words, metabolites are most abundant in the clinical groups with which they share a quadrant. Metabolites are colour-coded based on corresponding cluster as identified in **Figure 1** and according to the figure legend.
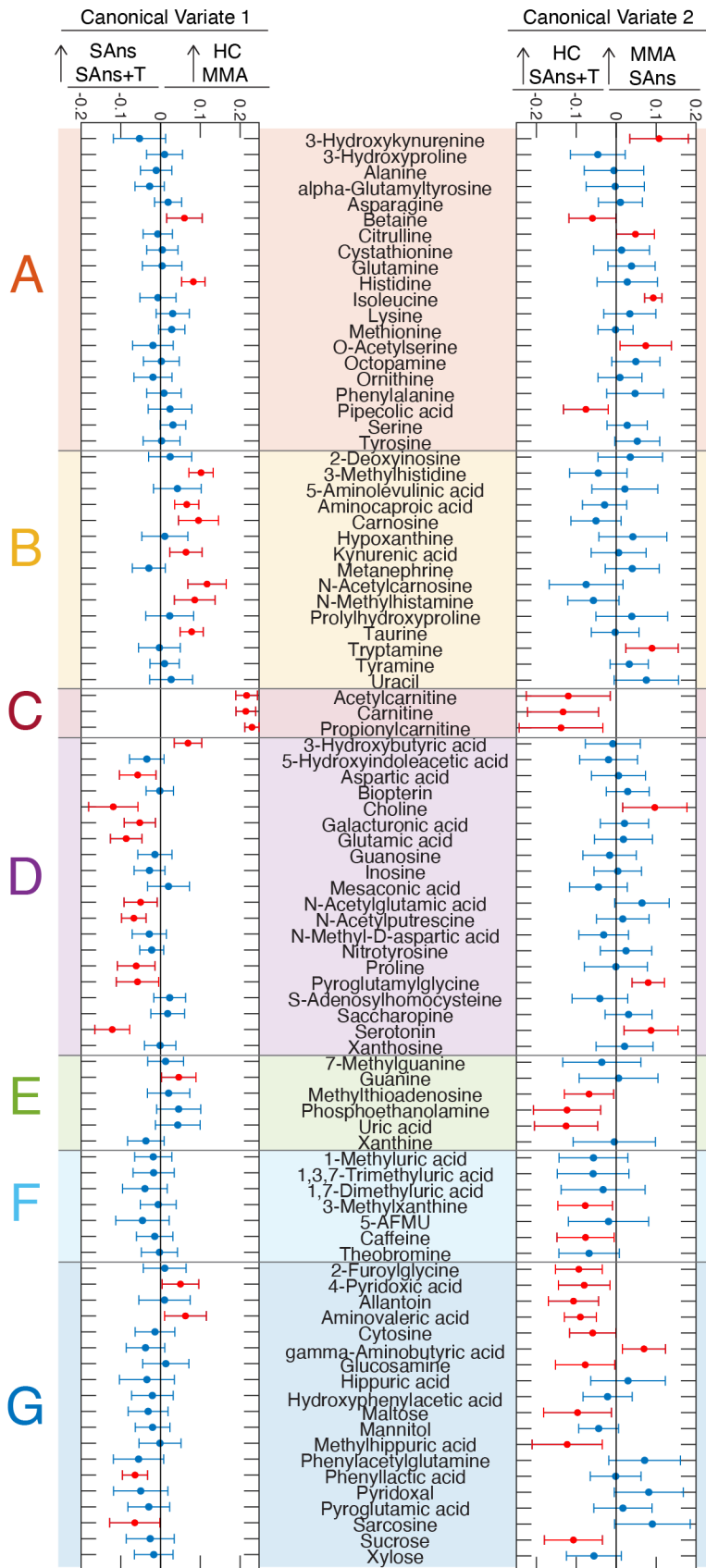
Figure E4. Individual Canonical Variate (CV) loadings for the PC-CVA with non-smoking severe asthmatics stratified by theophylline use. Loadings plots for Canonical Variate 1 (CV1, left panel) and CV2 (right panel) are shown. Red, metabolites that significantly (p<0.05) contribute to separation in the CV based on 500 iterations of bootstrap resampling / remodelling; blue, metabolites that do not significantly contribute to the separation in the CV. Metabolites are ordered and colour-coded by cluster as defined in **Figure 1**. The cluster label is presented on the left side of the figure. HC, healthy control participants; MMA, mild-to-moderate asthma; SAns, severe asthma non-smokers; SAs, severe asthma ex/smokers; T, theophylline.

(A) ... (box plots for Healthy Participants, MMA, SAns, SAs stratified by Male/Female with p-values p = 0.0001, p = 0.006, p = 0.002, p = 0.2)

(B) Males (p = 0.0027, p = 3.8 ×10⁻⁵) and Females (p = 0.0296)

(C)

Males

| | Baseline | | | | Longitudinal | |
	HC	MMA	SAns	SAs	SAns	SAs
Acetylcarnitine	1 (0.81,1.22)	0.77 (0.54,1.14)	0.53 (0.43,0.68)	0.58 (0.31,0.88)	0.52 (0.31,0.76)	0.84 (0.39,1.21)
Carnitine	1 (0.83,1.22)	1.05 (0.77,1.21)	0.73 (0.59,0.87)	0.8 (0.58,1.02)	0.75 (0.59,1.02)	0.84 (0.59,1)
Propionylcarnitine	1 (0.77,1.29)	0.72 (0.37,1.06)	0.49 (0.38,0.63)	0.38 (0.29,0.79)	0.5 (0.29,0.73)	0.66 (0.37,0.9)

Females

| | Baseline | | | | Longitudinal | |
	HC	MMA	SAns	SAs	SAns	SAs
Acetylcarnitine	1 (0.66,1.55)	0.69 (0.39,1.24)	0.47 (0.32,0.67)	0.58 (0.35,1.16)	0.53 (0.33,0.74)	0.59 (0.23,0.94)
Carnitine	1 (0.71,1.39)	1.02 (0.72,1.28)	0.84 (0.61,1)	0.94 (0.66,1.28)	0.87 (0.62,1.08)	0.97 (0.68,1.31)
Propionylcarnitine	1.01 (0.7,1.42)	0.95 (0.51,1.6)	0.6 (0.4,0.81)	0.62 (0.44,0.98)	0.66 (0.46,0.9)	0.66 (0.32,1.16)

Figure E5. Sex-specific differences in urinary carnitine levels. (A) The four U-BIOPRED groups stratified by sex. (**B)** The four U-BIOPRED groups compared separately for each sex. **C)** The fold-change estimates with 95% confidence intervals of the 3 carnitine species within each U-BIOPRED group stratified by sex relative to healthy participants. The urinary carnitine composite value was calculated by summing the log-transformed, z-scaled relative abundances of acetylcarnitine, carnitine, and propionylcarnitine. MMA, mild-to-moderate asthma; SAns, severe asthma non-smokers; SAs, severe asthma smokers and ex-smokers; SAnsL, severe asthma non-smokers longitudinal; SAsL, severe asthma smokers and ex-smokers longitudinal.
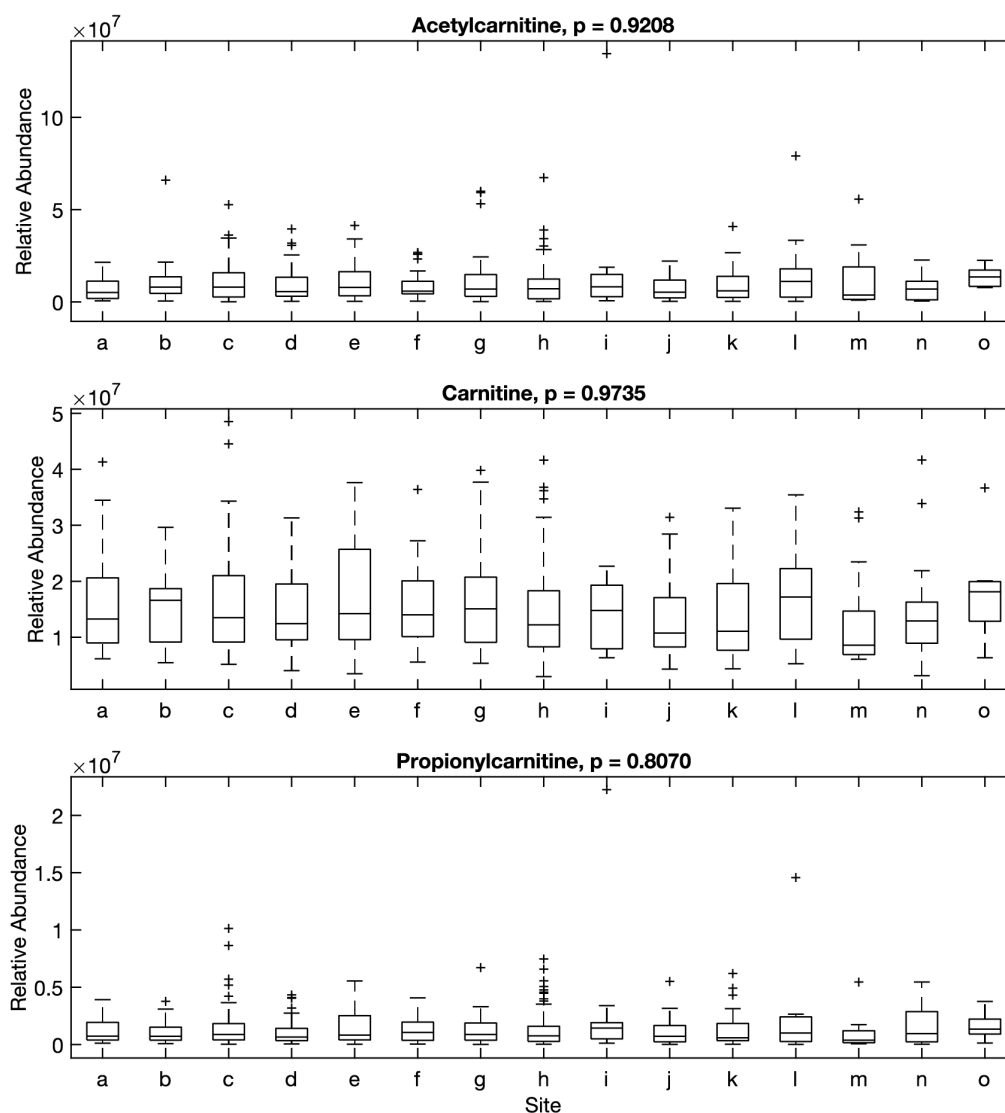
Figure E6. Dependency of urinary carnitine levels upon clinical recruitment site. The U-BIOPRED study consisted of 15 different patient recruitment sites across Europe. Boxplots are shown of the relative abundance of each carnitine metabolite stratified by clinical recruitment site code. Data are shown as post QC-corrected intensity values from the mass spectrometer in units of relative abundance. The Kruskal-Wallis p-values are reported in the figure.
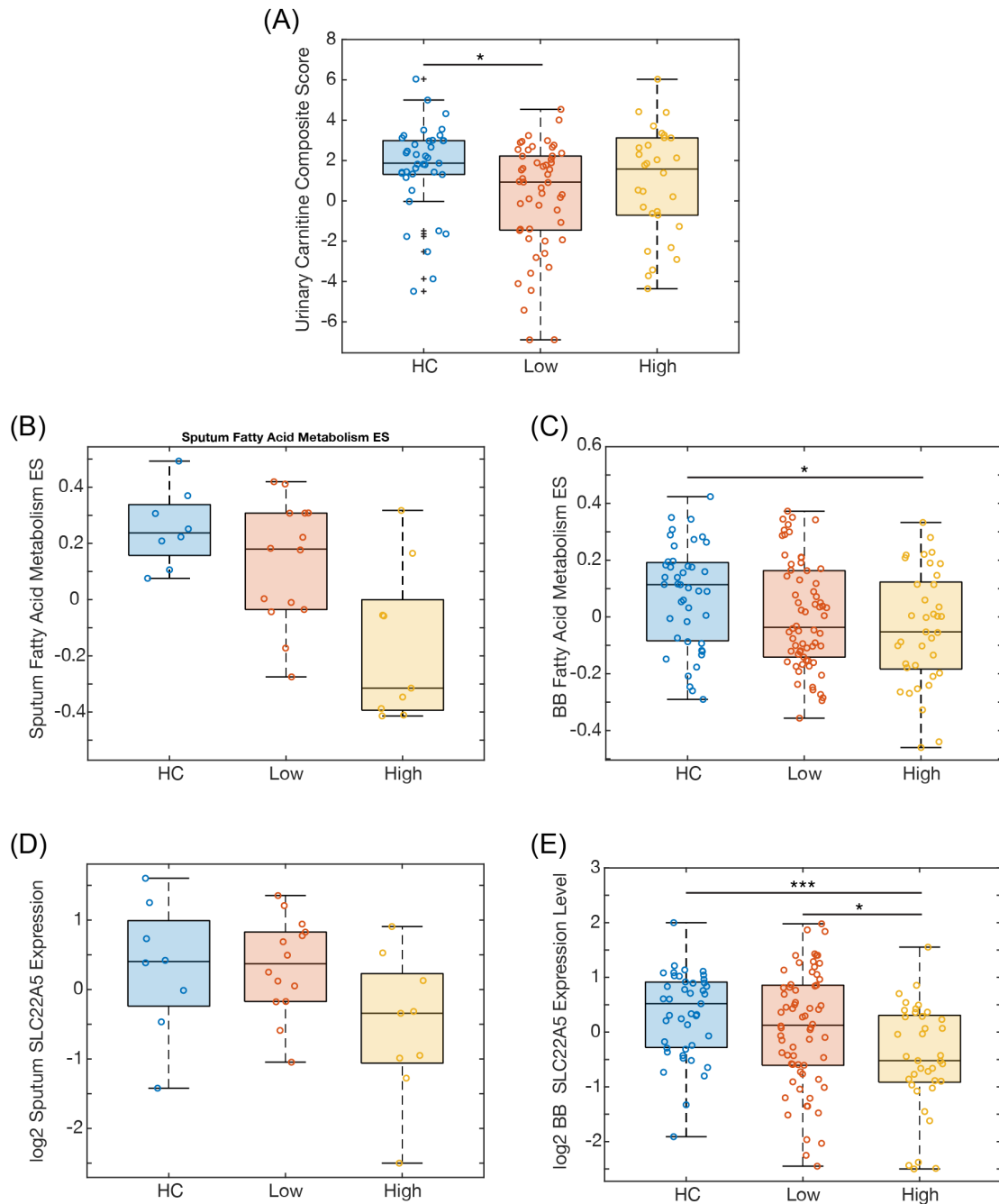
Figure E7. Molecular signatures of carnitine metabolism. Scatter-overlaid boxplots stratified by Type-2 classification. **(A)** Urinary carnitine composite variable. Relative abundances of carnitine, acetylcarnitine, and propionylcarnitine were log-transformed, z-scaled, and summed (p=0.031). **(B)** Sputum and **(C)** Bronchial brushings (BB) fatty acid metabolism enrichment score (ES) (p=0.038). **(D)** Sputum SLC22A5 expression levels. **(E)** Bronchial brushings (BB) SLC22A5 expression levels (p=9.7x10^{-4}). Inferential statistics were not performed for **(B)** and **(D)** due to small sample sizes. The Type-2 patient stratification was based on the ES of the IL-13-induced gene expression patterns in human bronchial epithelial cells using GSVA [23, 24]. Open circles, observations; box, median and interquartile range (IQR) of the data; whiskers, range of data up to 1.5 times of IQR above Q3 or below Q1; +, outliers. Kruskal-wallis p-values are reported, with posthoc pairwise comparisons shown on the figure. *, p<0.05; ***, p<0.001. HC, healthy control participants; Low, Type-2 low; High, Type-2 high.
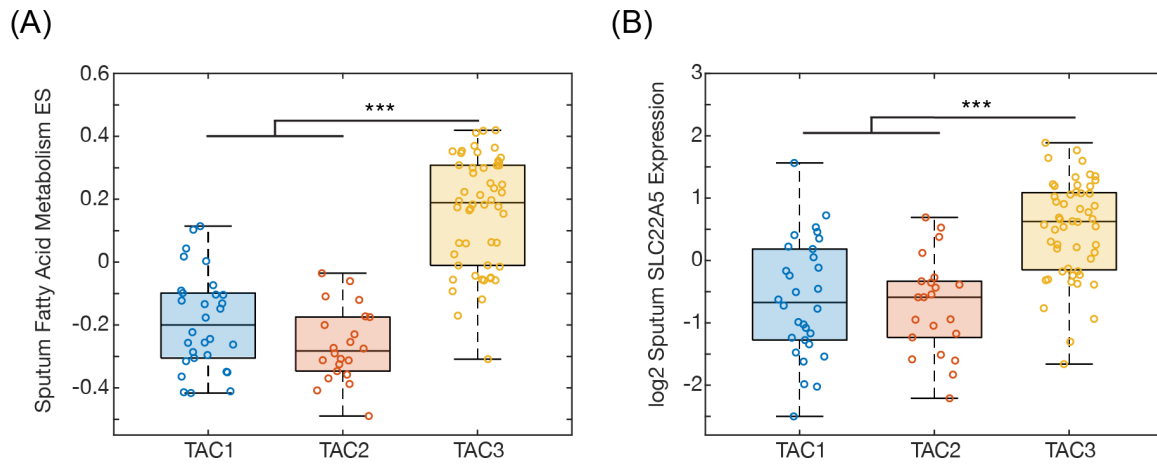
Figure E8. Molecular signatures of carnitine metabolism. Scatter-overlaid boxplots stratified by transcriptome-associated cluster (TAC) classification membership [23]. **(A)** Sputum fatty acid metabolism enrichment score (ES) ($p=2.1 \times 10^{-14}$). **(B)** Sputum SLC22A5 expression levels ($p=1.2 \times 10^{-8}$). Open circles, observations; box, median and interquartile range (IQR) of the data; whiskers, range of data up to 1.5 times of IQR above Q3 or below Q1; +, outliers. Kruskal-wallis p-values are reported here, with posthoc pairwise comparisons shown on the figure. ***, $p<0.001$.
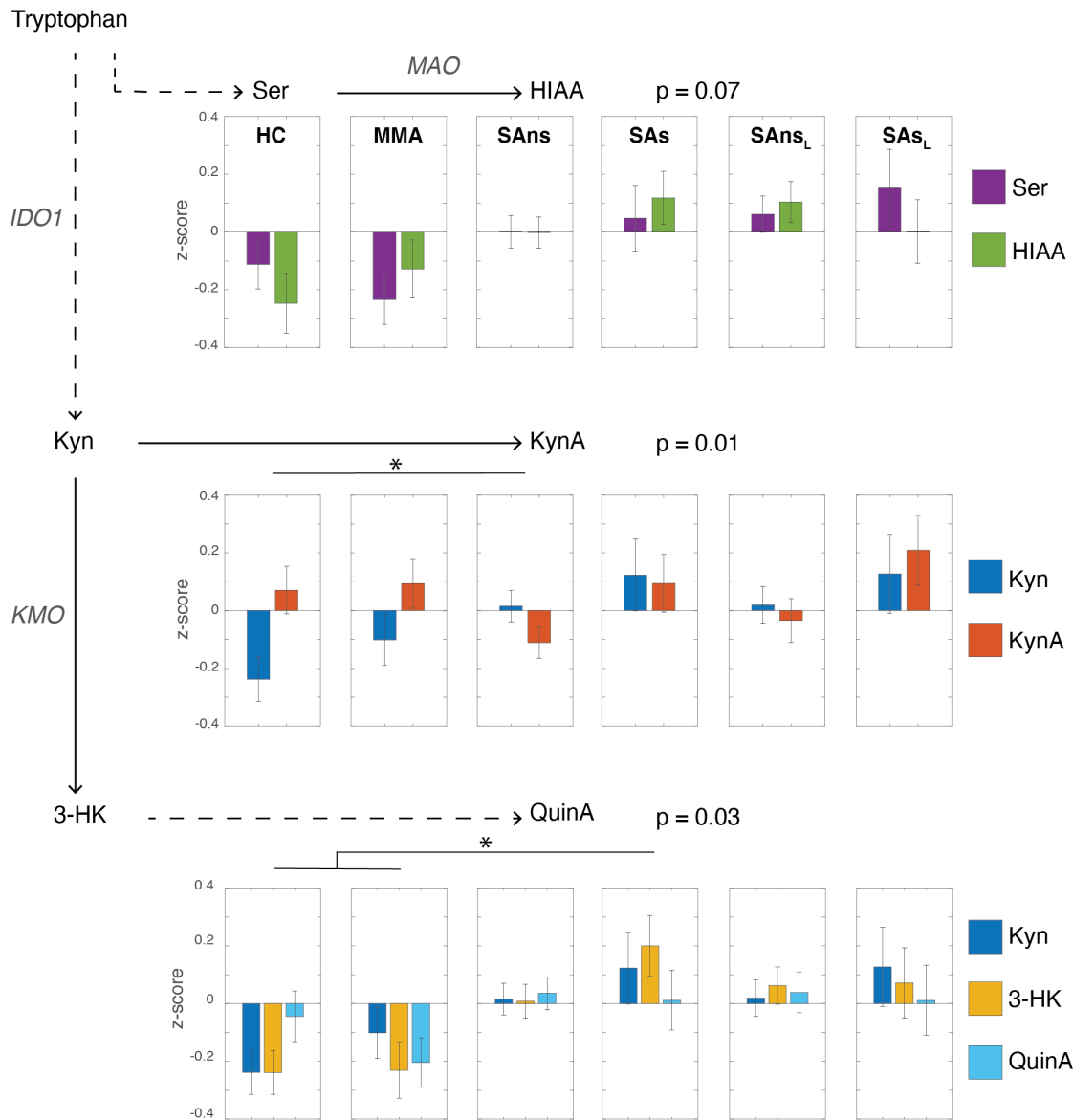
Figure E9. Tryptophan metabolism. Tryptophan and 6 downstream metabolites were quantified in urine and divided into 3 biochemical pathways: monoamine oxidase (MAO), indoleamine 2,3-dioxygenase (IDO), and kynurenine 3-monooxygenase (KMO). Downstream metabolites were normalised to tryptophan levels on an intra-individual basis, log-transformed, then z-scaled. To visualise and assess clinical group differences across each pathway, mean data were presented in a bar graph and MANOVA was performed. The quantified metabolite levels are provided in **Table E7**. Trp, tryptophan; Ser, serotonin; HIAA, 5-hydroxyindoleacetic acid; Kyn, kynurenine; KynA, kynurenic acid; QuinA, quinolinic acid. HC, healthy control participants; MMA, mild-to-moderate asthma; SAns, severe asthma non-smokers; SAs, severe asthma ex/smokers; L, longitudinal data.

References

1.   Shaw DE, Sousa AR, Fowler SJ, Fleming LJ, Roberts G, Corfield J, Pandis I, Bansal AT, Bel EH, Auffray C, Compton CH, Bisgaard H, Bucchioni E, Caruso M, Chanez P, Dahlen B, Dahlen SE, Dyson K, Frey U, Geiser T, Gerhardsson de Verdier M, Gibeon D, Guo YK, Hashimoto S, Hedlin G, Jeyasingham E, Hekking PP, Higenbottam T, Horvath I, Knox AJ, Krug N, Erpenbeck VJ, Larsson LX, Lazarinis N, Matthews JG, Middelveld R, Montuschi P, Musial J, Myles D, Pahus L, Sandstrom T, Seibold W, Singer F, Strandberg K, Vestbo J, Vissing N, von Garnier C, Adcock IM, Wagers S, Rowe A, Howarth P, Wagener AH, Djukanovic R, Sterk PJ, Chung KF, U-BIOPRED Study Group. Clinical and inflammatory characteristics of the European U-BIOPRED adult severe asthma cohort. *Eur Respir J* 2015: 46(5): 1308-1321.

2.   Kolmert J, Gomez C, Balgoma D, Sjodin M, Bood J, Konradsen JR, Ericsson M, Thorngren JO, James A, Mikus M, Sousa AR, Riley JH, Bates S, Bakke PS, Pandis I, Caruso M, Chanez P, Fowler SJ, Geiser T, Howarth P, Horvath I, Krug N, Montuschi P, Sanak M, Behndig A, Shaw DE, Knowles RG, Holweg CTJ, Wheelock AM, Dahlen B, Nordlund B, Alving K, Hedlin G, Chung KF, Adcock IM, Sterk PJ, Djukanovic R, Dahlen SE, Wheelock CE, U-BIOPRED Study Group. Urinary Leukotriene E4 and Prostaglandin D2 Metabolites Increase in Adult and Childhood Severe Asthma Characterized by Type 2 Inflammation. A Clinical Observational Study. *Am J Respir Crit Care Med* 2021: 203(1): 37-53.

3.   Naz S, Gallart-Ayala H, Reinke SN, Mathon C, Blankley R, Chaleckis R, Wheelock CE. Development of a Liquid Chromatography-High Resolution Mass Spectrometry Metabolomics Method with High Specificity for Metabolite Identification Using All Ion Fragmentation Acquisition. *Anal Chem* 2017: 89(15): 7933-7942.

4.   Dudzik D, Barbas-Bernardos C, Garcia A, Barbas C. Quality assurance procedures for mass spectrometry untargeted metabolomics. a review. *J Pharm Biomed Anal* 2018: 147: 149-173.

5.   Edmands WM, Ferrari P, Scalbert A. Normalization to specific gravity prior to analysis improves information recovery from high resolution mass spectrometry metabolomic profiles of human urine. *Anal Chem* 2014: 86(21): 10925-10931.

6.   Broadhurst D, Goodacre R, Reinke SN, Kuligowski J, Wilson ID, Lewis MR, Dunn WB. Guidelines and considerations for the use of system suitability and quality control samples in mass spectrometry assays applied in untargeted clinical metabolomic studies. *Metabolomics* 2018: 14(6): 72.

7.   Sumner LW, Amberg A, Barrett D, Beale MH, Beger R, Daykin CA, Fan TW, Fiehn O, Goodacre R, Griffin JL, Hankemeier T, Hardy N, Harnly J, Higashi R, Kopka J, Lane AN, Lindon JC, Marriott P, Nicholls AW, Reily MD, Thaden JJ, Viant MR. Proposed minimum reporting standards for chemical analysis Chemical Analysis Working Group (CAWG) Metabolomics Standards Initiative (MSI). *Metabolomics* 2007: 3(3): 211-221.

8.   Kirwan JA, Broadhurst DI, Davidson RL, Viant MR. Characterising and correcting batch variation in an automated direct infusion mass spectrometry (DIMS) metabolomics workflow. *Anal Bioanal Chem* 2013: 405(15): 5147-5157.

9.   Howie BN, Donnelly P, Marchini J. A flexible and accurate genotype imputation method for the next generation of genome-wide association studies. *PLoS Genet* 2009: 5(6): e1000529.

10.   Genomes Project Consortium, Auton A, Brooks LD, Durbin RM, Garrison EP, Kang HM, Korbel JO, Marchini JL, McCarthy S, McVean GA, Abecasis GR. A global reference for human genetic variation. *Nature* 2015: 526(7571): 68-74.

11.   Shabalin AA. Matrix eQTL: ultra fast eQTL analysis via large matrix operations. *Bioinformatics* 2012: 28(10): 1353-1358.

12.   Ferreira MAR, Mathur R, Vonk JM, Szwajda A, Brumpton B, Granell R, Brew BK, Ullemar V, Lu Y, Jiang Y, andMe Research T, e QC, Consortium B, Magnusson PKE, Karlsson R, Hinds DA, Paternoster L, Koppelman GH, Almqvist C. Genetic Architectures of Childhood- and Adult-Onset Asthma Are Partly Distinct. *Am J Hum Genet* 2019: 104(4): 665-684.

13.   Do KT, Wahl S, Raffler J, Molnos S, Laimighofer M, Adamski J, Suhre K, Strauch K, Peters A, Gieger C, Langenberg C, Stewart ID, Theis FJ, Grallert H, Kastenmuller G, Krumsiek J. Characterization of missing values in untargeted MS-based metabolomics data and evaluation of missing data handling strategies. *Metabolomics* 2018: 14(10): 128.

14.   Storey JD. A direct approach to false discovery rates. *Journal of the Royal Statistical Society: Series B (Statistical Methodology)* 2002: 64(3): 479-498.

15.   Hastie T, Tibshirani R, Friedman J. The Elements of Statistical Learning: Data Mining, Inference, and Prediction. 2nd ed. Springer, 2009.

16.   Reinke SN, Gallart-Ayala H, Gomez C, Checa A, Fauland A, Naz S, Kamleh MA, Djukanovic R, Hinks TS, Wheelock CE. Metabolomics analysis identifies different metabotypes of asthma severity. *Eur Respir J* 2017: 49(3).

17.   Huber PJ. The behavior of maximum likelihood estimates under nonstandard conditions. Proceedings of the Fifth Berkely Symposium on Mathematical Statistics and Probability, Volume 1: Statistics. University of California Press, Berkeley, California, 1967; pp. 221-233.

18.   Yeung AW, Terentis AC, King NJ, Thomas SR. Role of indoleamine 2,3-dioxygenase in health and disease. *Clin Sci (Lond)* 2015: 129(7): 601-672.

19.   Xu H, Oriss TB, Fei M, Henry AC, Melgert BN, Chen L, Mellor AL, Munn DH, Irvin CG, Ray P, Ray A. Indoleamine 2,3-dioxygenase in lung dendritic cells promotes Th2 responses and allergic inflammation. *Proc Natl Acad Sci U S A* 2008: 105(18): 6690-6695.

20.   Naz S, Bhat M, Stahl S, Forsslund H, Skold CM, Wheelock AM, Wheelock CE. Dysregulation of the Tryptophan Pathway Evidences Gender Differences in COPD. *Metabolites* 2019: 9(10).

21.   Gu F, Derkach A, Freedman ND, Landi MT, Albanes D, Weinstein SJ, Mondul AM, Matthews CE, Guertin KA, Xiao Q, Zheng W, Shu XO, Sampson JN, Moore SC, Caporaso NE. Cigarette smoking behaviour and blood metabolomics. *Int J Epidemiol* 2016: 45(5): 1421-1432.

22.   Budden KF, Shukla SD, Rehman SF, Bowerman KL, Keely S, Hugenholtz P, Armstrong-James DPH, Adcock IM, Chotirmall SH, Chung KF, Hansbro PM. Functional effects of the microbiota in chronic respiratory disease. *Lancet Respir Med* 2019: 7(10): 907-920.

23.   Kuo CS, Pavlidis S, Loza M, Baribaud F, Rowe A, Pandis I, Sousa A, Corfield J, Djukanovic R, Lutter R, Sterk PJ, Auffray C, Guo Y, Adcock IM, Chung KF, U-BIOPRED Study Group. T-helper cell type 2 (Th2) and non-Th2 molecular phenotypes of asthma using sputum transcriptomics in U-BIOPRED. *Eur Respir J* 2017: 49(2).

24.   Pavlidis S, Takahashi K, Ng Kee Kwong F, Xie J, Hoda U, Sun K, Elyasigomari V, Agapow P, Loza M, Baribaud F, Chanez P, Fowler SJ, Shaw DE, Fleming LJ, Howarth PH, Sousa AR, Corfield J, Auffray C, De Meulder B, Knowles R, Sterk PJ, Guo Y, Adcock IM, Djukanovic R, Fan Chung K, U-BIOPRED Study Group. "T2-high" in severe asthma related to blood eosinophil, exhaled nitric oxide and serum periostin. *Eur Respir J* 2019: 53(1).